Climate Dynamics (2025) 63:428
https://doi.org/10.1007/s00382-025-07913-3

The 5th generation regional climate modeling system, RegCM5: the first convection-permitting European wide simulation and validation over the CORDEX-CORE domains

Erika Coppola[1] · Filippo Giorgi[1] · Graziano Giuliani[1] · Emanuela Pichelli[9] · James M. Ciarlo[1,5] · Francesca Raffaele[1,7] · Rita Nogherotto[1,8] · Michelle Simões Reboita[1,2] · Chen Lu[1] · Natalia Zazulie[1,3] · Luiza Vargas-Heinz[1,4] · Andressa Andrade Cardoso[1,6] · Johannes de Leeuw[1,7]

Received: 21 October 2024 / Accepted: 4 October 2025 / Published online: 31 October 2025

Abstract

The Regional Climate Modeling system (RegCM) has undergone a significant evolution over the years, leading for example to the widely used versions RegCM4 and RegCM4-NH. In response to the demand for higher resolution, a new version of the system has been developed, RegCM5, incorporating the non-hydrostatic dynamical core of the MOLOCH weather prediction model. In this paper we assess the RegCM5's performance for 9 CORDEX-CORE domains, including a pan-European domain at convection-permitting resolution. We find temperature biases generally in the range of −2 to 2 °C, with a larger positive bias in the northernmost regions of North America and Asia during winter, linked to cloud water overestimation. There are cold biases over Central Asia and the Tibetan Plateau, possibly due to sparse station coverage. The model exhibits a prevailing cold bias in maximum temperature and warm bias in minimum temperature, associated with a systematic overestimation of lower-level cloud fraction, especially in winter. Taylor diagrams indicate a high spatial temperature pattern correlation with ERA5 and CRU data, except in South America and the Caribbean region. The precipitation evaluation shows an overestimation in South America, East Asia, and Africa. RegCM5 improves the daily precipitation distribution compared to RegCM4, particularly at high intensities. The analysis of wind fields confirms the model's ability to simulate monsoon circulations. The assessment of tropical cyclone tracks highlights a strong sensitivity to the tracking algorithms, thus necessitating a careful model interpretation. Over the European region, the convection permitting simulations especially improve the diurnal cycle of precipitation and the hourly precipitation intensities.

1 Introduction

Since the initial work of Dickinson et al. (1989) and Giorgi and Bates (1989) introducing the first version of the Regional Climate Modeling system (RegCM1), the dynamical downscaling technique using limited-area Regional Climate Models (RCMs) has become a well-known method used worldwide (Giorgi 2009). The RCM community has witnessed the evolution of various RCM systems, including subsequent model versions of the RegCM framework:

✉ Erika Coppola
coppolae@ictp.it

1 The Abdus Salam International Centre for Theoretical Physics, Trieste, Italy

2 Federal University of Itajubá, Itajubá, MG, Brazil

3 National Council of Scientific and Technical Research (CONICET), Buenos Aires, Argentina

4 Università degli Studi di Trieste, Trieste, Italy

5 University of Malta, Msida, Malta

6 Departamento de Ciências Atmosféricas, Instituto de Astronomia, Geofísica e Ciências Atmosféricas, Universidade de São Paulo, São Paulo, SP, Brazil

7 The National Institute of Oceanography and Applied Geophysics, Trieste, Italy

8 The Institute of Atmospheric Sciences and Climate (CNR-ISAC), Bologna, Italy

9 Climate Modeling and Impacts Laboratory (SSPT-MET-CLIM), ENEA - National Agency for New Technologies, Energy and Sustainable Economic Development, Rome, Italy

RegCM2, RegCM2.5, RegCM3, and the latest RegCM4 (Giorgi et al. 1993a, b; Giorgi & Mearns 1999; Pal et al. 2007; Giorgi et al. 2012). These model developments largely stemmed from the incorporation of new and more advanced physics packages, with the exception of the RegCM1 to RegCM2 transition, which brought an update to the model's dynamical core, adopting the MM5's hydrostatic dynamical representation (Grell et al. 1994).

RegCM4, in particular, has become a pivotal tool in the field, widely utilized across various projects and applications, ranging from process studies to paleo-climate research and future climate projections.This includes participation in the Coordinated Regional Downscaling Experiment (CORDEX, Giorgi et al. 2009; Gutowski et al. 2016). RegCM4 is designed to be coupled with ocean, land, chemistry, and aerosol modules in a fully interactive way, adding to its versatility (Sitz et al. 2017).

However, as the demand for higher spatial resolutions escalates, with the RCM community increasingly reaching "convection-permitting" resolutions of a few kilometers, RegCM4's hydrostatic dynamical core has been recognized as a limiting factor for such applications. As a result, the RegCM4 dynamical core underwent a significant upgrade, including the MM5 non-hydrostatic dynamics and leading to the development of RegCM4-NH (Coppola et al. 2021a). RegCM4-NH has already extensively been used for climate simulations at convection-permitting scales, e.g. within the European Climate Prediction System (EUCP) project and the CORDEX Flagship Pilot Study dedicated to convection (CORDEX-FPSCONV) (Coppola et al. 2020). Its potential has been demonstrated through multi-model experiments, including those carried out over the greater Alpine region by Ban et al. (2021) and Pichelli et al. (2021), over the South America region of La Plata basin (Betolli et al. 2021; da Rocha et al. 2024) and the region of Lake Victoria in Africa (Lipzig et al. 2023).

One of the major drawbacks of the RegCM4-NH is the computational cost to run the model, since the MM5 dynamical core is still based on a split explicit scheme requiring short time steps for stability constraints. In addition, the MM5 scheme includes a relatively high diffusion term, also to increase stability. For this reason, a new version of the RegCM modeling system, RegCM5 was developed by incorporating the dynamical core of the non-hydrostatic weather prediction model MOLOCH (Buzzi et al. 2014; Malguzzi et al. 2006; Trini Castelli et al. 2020) as part of a collaborative effort between the ICTP RegCM modeling team and the Institute of Atmospheric Sciences and Climate (ISAC) of the National Research Council (CNR) of Italy. The first version RegCM5 was introduced by Giorgi et al. (2023a, b), who tested it at 12 km resolution with parameterized convection and at convection permitting resolutions respectively over the Euro-CORDEX domain and the CORDEX FPS convection Alpine domain. In these experiments, the model was 4–5 times more computationally efficient than the old RegCM4 and RegCM4-NH counterparts: due to new dynamical core and enhanced stability, longer timesteps can be used. Moreover, some computational resources are saved because no shallow cumulus scheme triggering is no longer required. This means that for the same domain configuration and computational resources, longer simulations can be run.

Furthermore, RegCM5 improved different aspects of model performance, in particular the occurrence of extreme precipitation events and some systematic temperature biases (Giorgi et al. 2023a).

RegCM5 thus represents an important step forward for model users, in particular when using the model at very high spatial resolutions. It is important to acknowledge that the success of the RegCM system is not only the work of the core development teams, but also a result of contributions from the broader user community, who play a vital role in testing the model, identifying errors, customizing model configurations, and implementing new components. As RegCM5 has become available for public use, ongoing feedback and optimization efforts from prospective users will continue to refine the model's performance and applicability. This is especially important in view of the fact that the RegCM system includes multiple representations of different physics processes, which can be quite sensitive to the region of application.

For this reason, it is very helpful to provide model users with some basic information of the performance of a standard version of the model optimized over a variety of climate conditions, which can then provide the basis of more detailed customizations for different applications. Therefore, in this paper we extend the analysis of Giorgi et al. (2023a) by presenting a version of the model optimized and tested over nine domains used in the CORDEX-CORE effort (Giorgi et al. 2022; Teichmann et al. 2021; Coppola et al. 2021b), along with a convection-permitting experiment covering for the first time the entire European region. A number of different aspects of model performance are assessed using a variety of observation datasets for model validation, and for all experiments the model is driven at the lateral boundaries by reanalyses of observations.

We first present in Sect. 2 a brief summary of the main model features, the methodology and setting for the simulations reported in Sect. 3, results are discussed in Sect. 4 and summary and future outlooks are provided in Sect. 5.

2 RegCM5 model description

RegCM5 includes both hydrostatic and non-hydrostatic dynamical cores, as well as a wide range of physics options. It can be employed as a limited area model for any region globally or using a tropical band configuration (Coppola et al. 2012). The significant enhancement in RegCM5 compared to the previous version RegCM4 is the integration of the non-hydrostatic dynamical core from the MOLOCH weather prediction model, along with some upgrades to the model physics.

The MOLOCH dynamical core used in RegCM5 is described by Giorgi et al. (2023a) and references therein. It uses a hybrid terrain-following uniform vertical coordinate and an Arakawa and Lamb C horizontal grid with uniform spacing and staggered wind components.

The model equations are expressed in terms of the variables $(T,\ P,\ \Pi,\ \Theta,\ u,\ v,\ w,\ q,\ T_v)$, where

T is the temperature
P is the pressure
$q_v,\ q_c,\ q_i$ are the mass mixing ratio of water vapor, liquid water and ice water
$\Pi = \left(\frac{P}{P_0}\right)^{\frac{R_d}{C_{p_d}}}$ is the Exner function
$\Theta_v = \frac{T_v}{\Pi}$ is the virtual potential temperature and

$T_v \approx T\,(1 + 0.61 q_v - q_c - q_i)$ is the virtual temperature
u, v are the zonal and meridional components of the wind
w is the vertical component of the wind

The prognostic equations for Π and Θ_v are a good approximation of the exact thermodynamic and continuity equation of moist air. The horizontal and vertical derivatives are computed using a second order, centered finite difference scheme, while the time integration follows a three-step explicit scheme: vertical sound wave propagation with an implicit Euler-backward scheme with time step dt_s, advection terms with a second-order total variation method with time step dt_a, and physical parameterization terms added with a user-configured large time step dt_p. The dt_a and dt_s time steps are integer fractions of dt_p, i.e.

$$dt_a = \frac{dt_p}{n_{adv}}, dt_s = \frac{dt_a}{n_{sound}}$$

with n_{sound} and n_{adv} being user configurable parameters. The generalized vertical velocity is zero at the surface and at the model top. No explicit diffusion is required and numerical stability is attained by applying a second order spatial filter on the divergence of the horizontal wind with a user configurable coefficient.

For further technical details we refer to Giorgi et al. (2023a) and Malguzzi et al. (2006) who provide comprehensive information on the model equations and solution procedures.

A summary of the additional features available in the new RegCM5 model version optimized over the CORDEX-CORE domains is reported in Table 1.

3 Methods

The RegCM5 model has been tested over the entire set of CORDEX-CORE domains (see Fig. S1 in the Supplementary Material), which were previously simulated with the RegCM4.7 version (Coppola et al. 2021a; Giorgi et al. 2022). Additionally, the model was tested for the first time at a convection-permitting (CP) resolution over a pan-European domain. For each domain, multiple observations and reanalysis data have been utilized for model assessment, as reported in Table 2.

All simulations use ERA5 reanalysis fields (Hersbach et al. 2020) as initial and lateral boundary conditions. Specific model configurations for each domain, including spatial resolution and the simulation period, are provided in Table 3. A number of 30 levels has been chosen for the vertical resolution, being a good compromise between vertical details and computational time. The high resolution simulation at 3 km over Europe is the only one to have 50 vertical levels to balance the higher horizontal resolution and keeping the the top of the atmosphere at the same height.

The model validation was conducted over the set of subregions identified in the AR6 WGI IPCC report covered by the RegCM5 domains The regions are described by Iturbide et al. (2020). Various metrics were computed to validate the model, encompassing both mean climate and extreme climate distribution, as shown in Table 4.

3.1 Mean seasonal bias

The mean seasonal bias for 2 m, mean, maximum and minimum temperature (T_{mean}, T_{max}, and T_{min} respectively), mean precipitation (pr), precipitation intensity and frequency (pr-int and pr-frq), as well as the annual 99th percentile (p99), were used for the validation of the model mean climatology (definition of the metrics can be found in Table 4). For temperature, the model results are compared with observations from the Climate Research Unit (CRU) dataset. For mean precipitation, the reference dataset is the Global Precipitation Climatology Centre (GPCC), and for precipitation intensity/frequency and p99 the Climate Prediction

Table 1 Dynamics, physics and coupled component options available in RegCM5

Model aspects	Available options
Dynamics	Hydrostatic, vertical pressure coordinate (Giorgi et al. 1993a) Non-hydrostatic, vertical pressure coordinate (Coppola et al. 2012) Non-hydrostatic, height based coordinate (MOLOCH, Malguzzi et al. 2006; Davolio et al. 2020)
Radiative transfer	Modified CCM3 (Kiehl et al. 1996) RRTM (Mlawer et al. 1997a, 1997b)
Planetary boundary layer	Modified Holtslag (Holtslag et al. 1990) UW-PBL (Bretherton et al. 2004)
Cumulus convection	Simplified Kuo (Anthes et al. 1987, not available for MOLOCH dynamics) Grell (Grell 1993) MIT (Emanuel and Zivkovic-Rothman 1999) Tiedtke (Tiedtke 1989) Kain-Fritsch (Kain 2004)
Resolved scale precipitation	SUBEX (Pal et al. 2000) WRF-single-moment-microphysics classes 5 (Hong et al. 2004) Nogherotto-Tompkins (Nogherotto et al. 2016)
Cloud fraction	**Sundqvist** (Sundqvist 1988) **Xu and Randall** (1996) **Both modified according to Liang and Wu** (2005)
Land surface	BATS (Dickinson et al. 1993) CLM3.5 (Steiner et al. 2009) CLM4.5 (Oleson et al. 2013) Sub-grid BATS (Giorgi et al. 2003) and CLM4.5
Land use	**Dynamical land use forcing from LUCAS LUC V1.1, based on LUH2 (Hoffmann et al.2022) for the European Domain**
Ocean fluxes	BATS (Dickinson et al. 1993) Zeng (Zeng et al. 1998) COARE (Fairall et al. 2003) Diurnal sea surface temperature (Zeng and Beljaars 2005)
Aerosols radiative effect	Organic and black carbon, SO4 (Solmon et al. 2006, 2008) Dust (Zakey et al. 2006) Sea salt (Zakey et al. 2008) Gas-phase (Shalaby et al. 2012) Pollen (Liu et al. 2016) **Implementation of Global Aerosol OPP Profile Reanalysis from MERRA-2 (Gelaro et al.**2017, last version available at: https://doi.org/10.34730/bc801a23b8bf48e98a50e23e909bf19c), **but only with one optical band (visible)**
Interactive lake	1D diffusion/convection (Hostetler et al. 1993)
Interactive vegetation	CLM4.5 CNDV (Shi et al. 2018)
Tropical band	(Coppola et al. 2012)
Coupling	RegCM-ES (Sitz et al. 2017) ROMS Ocean (Ratnam et al. 2009) MIT GCM Ocean (Artale et al. 2010) ChyM hydrology (Di Sante et al. 2019) BFM biogeochemical (Reale et al. 2020)
Sea ice	BATS (Dickinson et al. 1993)
IPCC forcing	AR4 GHG (CMIP3: A1B, A2, B1, B2) AR5 GHG (CMIP5: RPC2.6, RCP4.5, RCP6.0, RCP8.5) AR6 GHG (CMIP6: SSP119, SSP126, SSP245, SSP370, SSP434, SSP460, SSP534, SSP585) SPARC SOLARIS HEPPA irradiances SPARC CCMI Ozone Anthropogenic aerosol simple plume model

Bold letters highlight the options newly available since the RegCM5 version described by Giorgi et al. (2023a)

Center (CPC) is used as reference. The seasonal means are first calculated over the baseline period (1980 to 2010 for Europe and 2000 to 2009 for all other domains) at the original resolutions and are subsequently interpolated (distance-weighted average for temperature, and nearest neighbour for precipitation and related metrics) to the resolution of the observations. The area-weighted averages of all variables are then computed over the AR6 WGI IPCC regions contained within each domain, and the biases are then derived by taking the difference between the simulated and observed

Table 2 Observational datasets

Observed datasets	Domain	Variables	Data type	Spatial resolution	Temporal resolution	Period	References
CPC_Global	Global Land	PRECIP TMAX TMIN	Gridded, Station based	0.50 degrees	DAILY	1979–2021	Chen et al. (2008)
TRMM	Tropics	PRECIP	Satellite observation based	0.25 degrees	3-HOURLY	1998–2017	Kummerow et al. (2000)
MSWEP	Global	PRECIP	Derived by optimally merging a range of gauge, satellite, and reanalysis estimates	0.10 degrees	DAILY	1979–2020	Beck et al. (2019)
GPCC	Global	PRECIP	Gridded, Station based	0.25 degrees	MONTHLY	1891–2020	Schneider et al. (2022
GPCC	Global	PRECIP	Gridded, Station based	1.0	DAILY	1982–2020	Schamm et al. (2014)
CRU	Global Land	PRECIP TMEAN	Station based	0.50 degrees	MONTHLY	1901–2015	Harris et al. (2020)
APHRO	India and East Asia	PRECIP	Grid	0.25 degrees	DAILY	1951–2007	Yatagai et al. (2009)
E_OBS	Europe Land	PRECIP TMAX TMIN	Grid	0.25 degrees	DAILY	1950–2015	Cornes et al. (2018)
CN05.1	China	PRECIP TMEAN	Station based	0.25 degrees	DAILY	1961–2012	Wu and Gao (2013)
ERA5	Global	WIND, PRECIP, CLOUD FRACTION, CLOUD WATER, CLOUD ICE, MEAN SEA LEVEL PRESSURE, TMEAN	Reanalysis	0.25 degrees	HOURLY	1940–Present	Hersbach et al. (2020)
IBTrACS	Global	TROPICAL CYCLONES TRACK	Merging datasets from different agencies	–	DAILY	1842–Present	Knapp et al. (2010, 2018)
REGNIE	Germany	PRECIP	Station based	1 km	DAILY	1961–2014	Rauthe et al.(2013)
RADKLIM	Germany	PRECIP	Radar based (rain gauges calibration)	1 km	HOURLY	2001–2009	Kreklow et al. (2020)
SPAIN02	Spain	PRECIP	Station based	0.11 degrees	DAILY	1971–2010	Herrera et al. (2010)
CARPATCLIM	Carpatians	PRECIP	Station based	0.1 degrees	DAILY	1961–2010	Szalai et al. (2013)
ENG_REGR	Great Britain	PRECIP	Station based	5 km	DAILY	1990–2010	http://www.precisrcm.com/Erasmo/ncic.uk.11.tgz
COMEPHORE	France	PRECIP	Reanalysis based on radar and rain gauges	1 km	HOURLY	1997–2017	Tabary et al. (2012)
GRIPHO	Italy	PRECIP	Station based gridded dataset	3 km	HOURLY	2001–2016	Fantini (2019)
EURO4M	Alps	PRECIP	Station based gridded dataset	5 km	DAILY	1971–2008	Isotta et al. (2014a)
PTHBV	Sweden	PRECIP	Station based gridded dataset	4 km	DAILY	1961–2011	https://opendata-download-metanalys.smhi.se Johansson (2000)
METNO	Norway	PRECIP	Station based gridded dataset	1 km	DAILY	1980–2008	Mohr et al. (2009)
RdisaggH	Switzerland	PRECIP	Combination of rain-gauge data and radar measurements	1 km	HOURLY	2003–2010	Wüest et al. (2010)
CEH-GEAR	Great Britain	PRECIP	Rain-gauge based gridded dataset	1 km	HOURLY	1990–2016	Lewis et al. (2022)

Table 3 Model configuration for each domain

DOMAIN	Period	Horizontal Resolution	Vertical Resolution (Ztop)	Boundary Layer Scheme (ib ltyp)	Cumulus convection scheme (icup_lnd/ocn)	Moisture scheme (ipptis)	Cloud fraction algorithm (icldfrac)	Dynamical land use
Australasia	2000–2009	25 km	30 levels (30 km)	Holtslag PBL	Tiedtke/Tiedtke	Explicit moisture Nogherotto/Tompkins	SUBEX	NO
East Asia	2000–2009	25 km	30 levels (30 km)	Holtslag PBL	Tiedtke/Tiedtke	Explicit moisture Nogherotto/Tompkins	Xu-Randall empirical	NO
South East Asia	2000–2009	25 km	30 levels (30 km)	Holtslag PBL	Tiedtke/Tiedtke	Explicit moisture Nogherotto/Tompkins	SUBEX	NO
South America	2000–2009	25 km	30 levels (30 km)	Holtslag PBL	Tiedtke/Tiedtke	Explicit moisture Nogherotto/Tompkins	SUBEX	NO
Central America	2000–2009	25 km	30 levels (30 km)	Holtslag PBL	Tiedtke/Tiedtke	Explicit moisture Nogherotto/Tompkins	SUBEX	NO
Europe	2000–2009	3 km	50 levels (30 km)	Holtslag PBL	None/None	Explicit moisture Nogherotto/Tompkins	Xu-Randall empirical	NO
	1980–2010	12 km	30 levels (30 km)	Holtslag PBL	Tiedtke/Tiedtke	Explicit moisture Nogherotto/Tompkins	Xu-Randall empirical	YES
South Asia	2000–2009	25 km	30 levels (30 km)	Holtslag PBL	Tiedtke/Tiedtke	Explicit moisture Nogherotto/Tompkins	Xu-Randall empirical	NO
North America	2000–2009	25 km	30 levels (30 km)	Holtslag PBL	Tiedtke/Tiedtke	Explicit moisture Nogherotto/Tompkins	Xu-Randall empirical	NO
Africa	200–2009	25 km	30 levels (30 km)	Holtslag PBL	Tiedtke/Tiedtke	Explicit moisture Nogherotto/Tompkins	SUBEX	NO

Table 4 Metrics used for model validation

Metric	Definition	Unit
T_{mean}	Daily mean 2-m temperature	°C
T_{max}	Daily maximum 2-m temperature	°C
T_{min}	Daily minimum 2-m temperature	°C
pr	Daily/hourly total precipitation	mm/day, mm/hr
pr-frq	Total number of wet days/hours (i.e., days/hours with total precipitation greater than 1/0.5 mm)	day/year
pr-int	Average amount of wet-day and wet-hour precipitation	mm/day, mm/hr
p99	The 99th percentile of the precipitation distribution over the time period considered	mm/day, mm/hr
p99.9	The 99.9th percentile of the precipitation distribution over the time period considered	mm/day, mm/hr
cl	Cloud fraction	%
clw	Cloud liquid water	mg/kg
cli	Cloud ice	mg/kg

values. The mean bias over all the regions is obtained in the same way, except that the area-weighted average is calculated over all grids of all domains.

3.2 Precipitation distribution

Boxplots were computed for daily precipitation in all regions considered, from RegCM4, RegCM5 and observations. We use the station-based data from CPC except for Europe, for which the observation dataset is E-OBS. Due to the steepness of the distribution, the box plots include the 5th and 95th and 99th percentiles.

Note that over some regions, and particularly the Mediterranean, RegCM4 exhibited a notable overestimation of extreme events due to the occurrence of numerical grid point storms, a problem that is considerably improved in RegCM5. Therefore, in the box plots, events with excessively large amounts in RegCM4 were excluded by adjusting the figure axes limits to align with the distribution from observations and RegCM5.

Hourly precipitation distributions for the period 2000–2009 were calculated for the RegCM5 CP and 12 km simulation over Europe and compared with high-resolution hourly observations over Italy, Switzerland, Germany, France and Great Britain (see Table 2). Furthermore, results were compared with the ERA5 reanalysis estimates. Distributions are calculated by taking all available time steps and grid points within each dataset considered. Some of the observational datasets did not have observations at the start of the RegCM5 simulations (e.g. Switzerland observational dataset starts in 2003). Therefore, in order to consider a consistent time period for the observations and model simulations, we used the first five available years for each of the observational datasets (e.g. Switzerland 2003–2007).

Daily precipitation distributions are calculated for 2000–2009 for the Europe RegCM5 model simulations, ERA5 and all available observations in the simulated region. In addition to the observational datasets mentioned above, daily precipitation estimates from Sweden, Norway, Spain

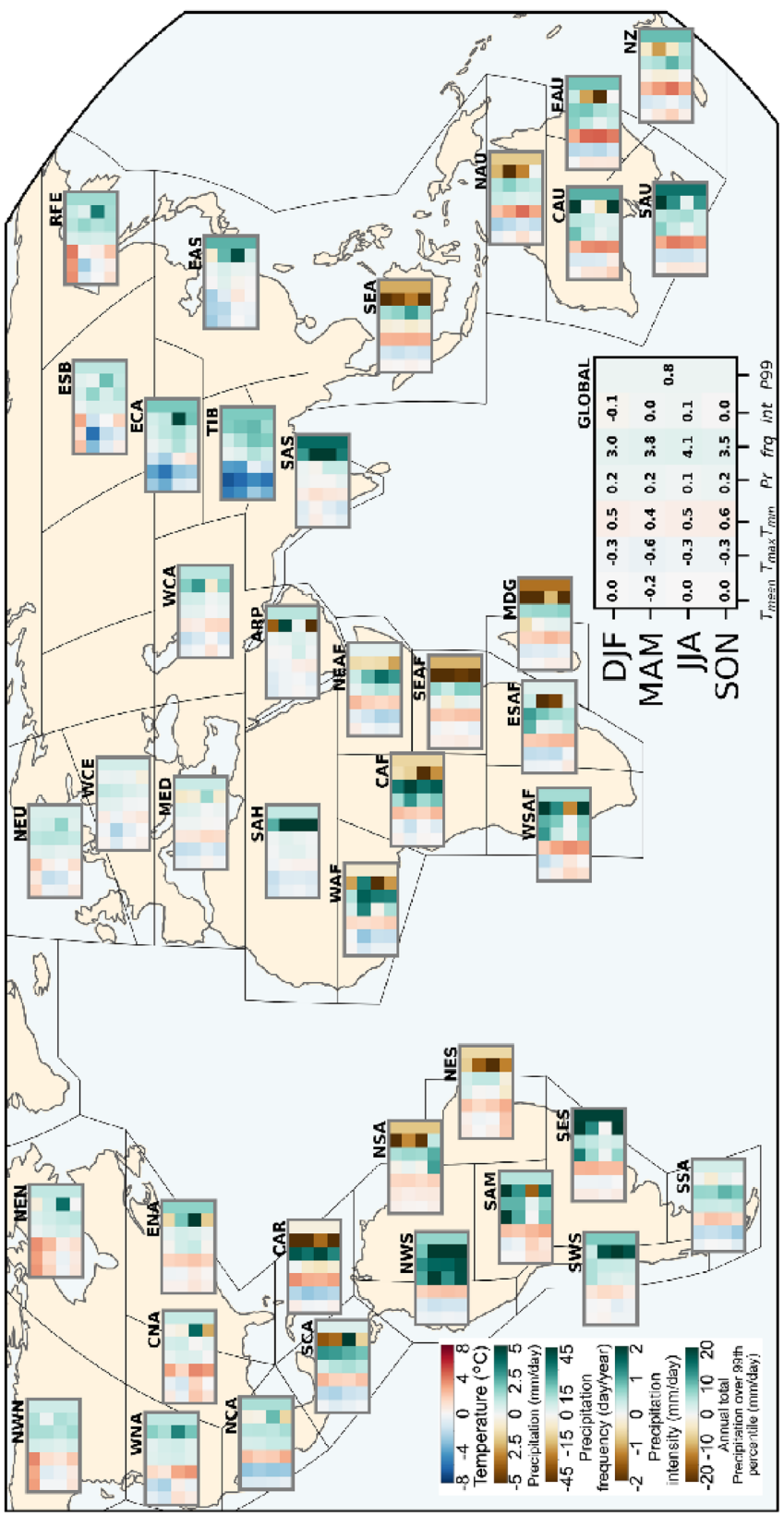

NWN	N.W.North-America	NES	N.E.South-America	CAF	Central-Africa	TIB	Tibetan-Plateau
NEN	N.E.North-America	SAM	South-America-Monsoon	NEAF	N.Eastern-Africa	EAS	E.Asia
WNA	W.North-America	SWS	S.W.South-America	SEAF	So.Eastern-Africa	ARP	Arabian-Peninsula
CNA	C.North-America	SES	S.E.South-America	WSAF	W.Southern-Africa	SAS	S.Asia
ENA	E.North-America	SSA	S.S.South-America	ESAF	E.Southern-Africa	SEA	S.E.Asia
NCA	N.Central-America	NEU	N.Europe	MDG	Madagascar	NAU	N.Australia
SCA	S.Central-America	WCE	Western&Central-Europe	ESB	E.Siberia	CAU	C.Australia
CAR	Caribbean	MED	Mediterranean	RFE	Russian-Far-East	EAU	E.Australia
NWS	N.W.South-America	SAH	Sahara	WCA	W.C.Asia	SAU	S.Australia
NSA	N.South-America	WAF	Western-Africa	ECA	E.C.Asia	NZ	New-Zealand

Fig. 1 Mean seasonal bias of each region for Tmean, Tmin, Tmax, pr, pr-frq, pr-int and the annual value of p99. The period covered is 2000–2009, except for the European domain (MED, WCE and NEU regions): 1980–2010. A global mean season bias table with its respective values has been added to the figure

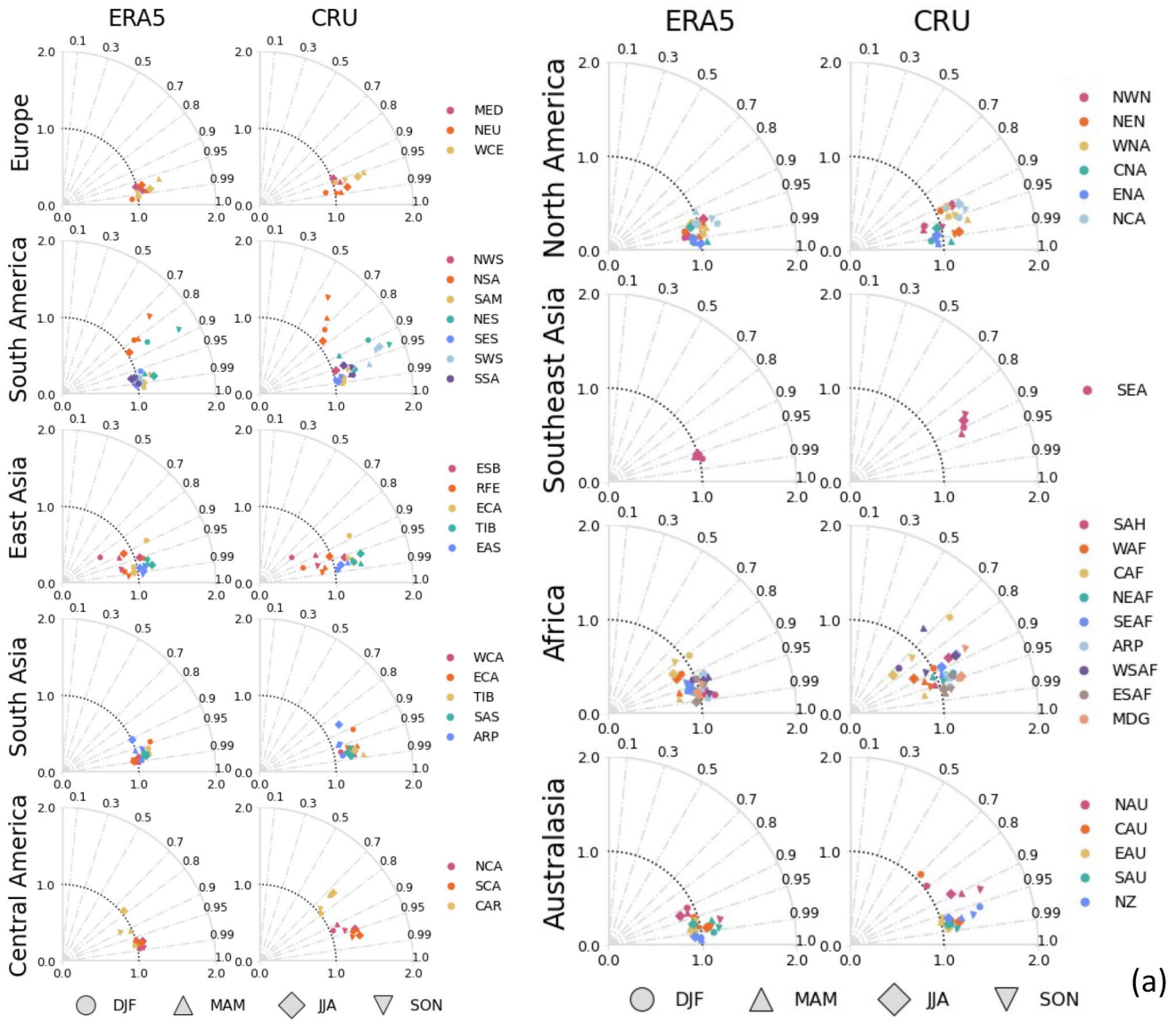

Fig. 2 Taylor diagrams for the mean temperature (panel a) and precipitation (panel b) for selected domains and datasets. Symbols represent seasons and colors are the subregions of a specific domain

and the Carpatians are also available (see Table 2). All the biases were computed interpolating each observational dataset on the model grid.

3.3 Precipitation sub daily analysis

Seasonal diurnal cycles of precipitation were computed for Europe, analysing both the 12 km and the 3 km simulations. The comparison was carried out against ERA5 data as well as different sub-regional hourly observation datasets: GRIPHO (Italy), RdisaggH (Switzerland), RADKLIM (Germany), COMEPHORE (France) and CEH-GEAR (Great Britain). Each high-resolution dataset was interpolated on the coarser model grid and the daily cycle was computed spatially averaging only in the region covered by observations.

Precipitation intensity and frequency for the hourly observation and RegCM5 datasets were calculated using hourly minimum precipitation thresholds of 0.1 mm/hr and 0.5 mm/hr in order to investigate the uncertainties in the data at very low intensities, which can strongly influence the biases. Note that the choice of threshold does not influence the p99.9 estimates as the whole distribution (including dry hours) is used to calculate this variable.

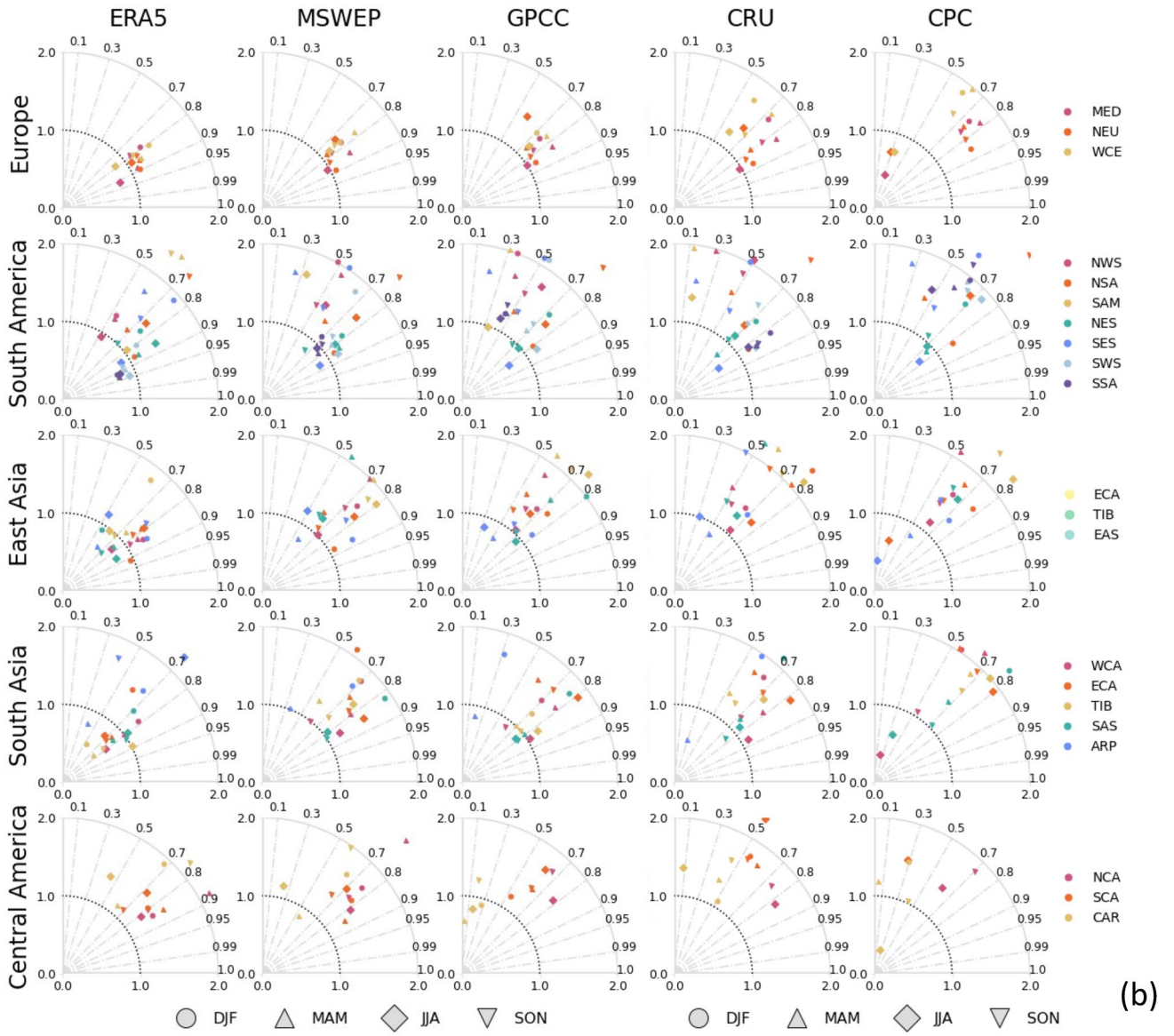

Fig. 2 (continued)

3.4 Taylor diagram

Taylor diagrams were used to validate the mean seasonal precipitation and temperature against several reference datasets. For precipitation, the model results are compared with ERA5, CRU, MSWEP, CPC, and GPCC. For temperature, ERA5 and CRU are used, except for additional observation datasets for Europe and East Asia. Specifically, for Europe, precipitation and daily mean temperature are compared against E-OBS, while for several subregions of East Asia, they are compared against APHRO and CN05.1. For each subregion, the gridded seasonal averages of the observed and simulated data are used to calculate the area-weighted centered pattern correlation and the ratio between the simulated and observed standard deviations, which are then used to generate the diagrams.

3.5 Cloud distributions

Vertical profiles were computed over each region for the mean seasonal cloud fraction, cloud liquid water and cloud ice in June–July–August (JJA) and December–January–February (DJF) using twelve pressure levels: 1000, 925, 850, 700, 600, 500, 400, 300, 250, 200, 150 and 100 hPa. The calculations were done for both RegCM5 and the ERA5 reanalysis data and covered the period 2000–2009 for all domains, except for Europe, for which 1980–2010 was used.

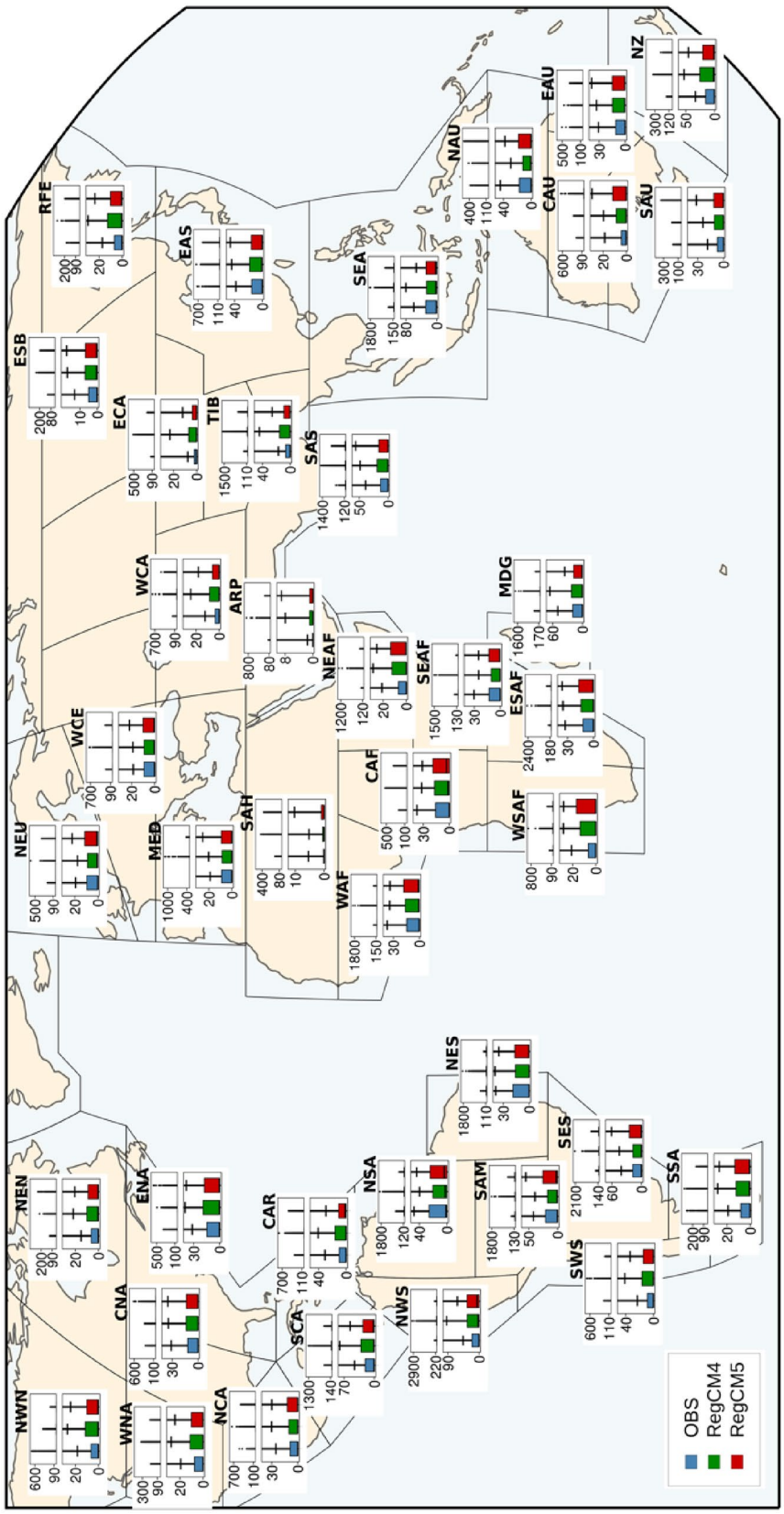

Fig. 3 Boxplot of daily precipitation for the period 2000–2009, except for the European domain (MED, WCE and NEU regions): 1980–2010. Colored boxes are limited by the 5th and 95th percentile. The upper black bar indicates the 99th percentile. Blue boxes correspond to the observations from CPC, except for the European domain: EOBS. Green boxes indicate RegCM4 and red boxes, RegCM5. Units are mm per day

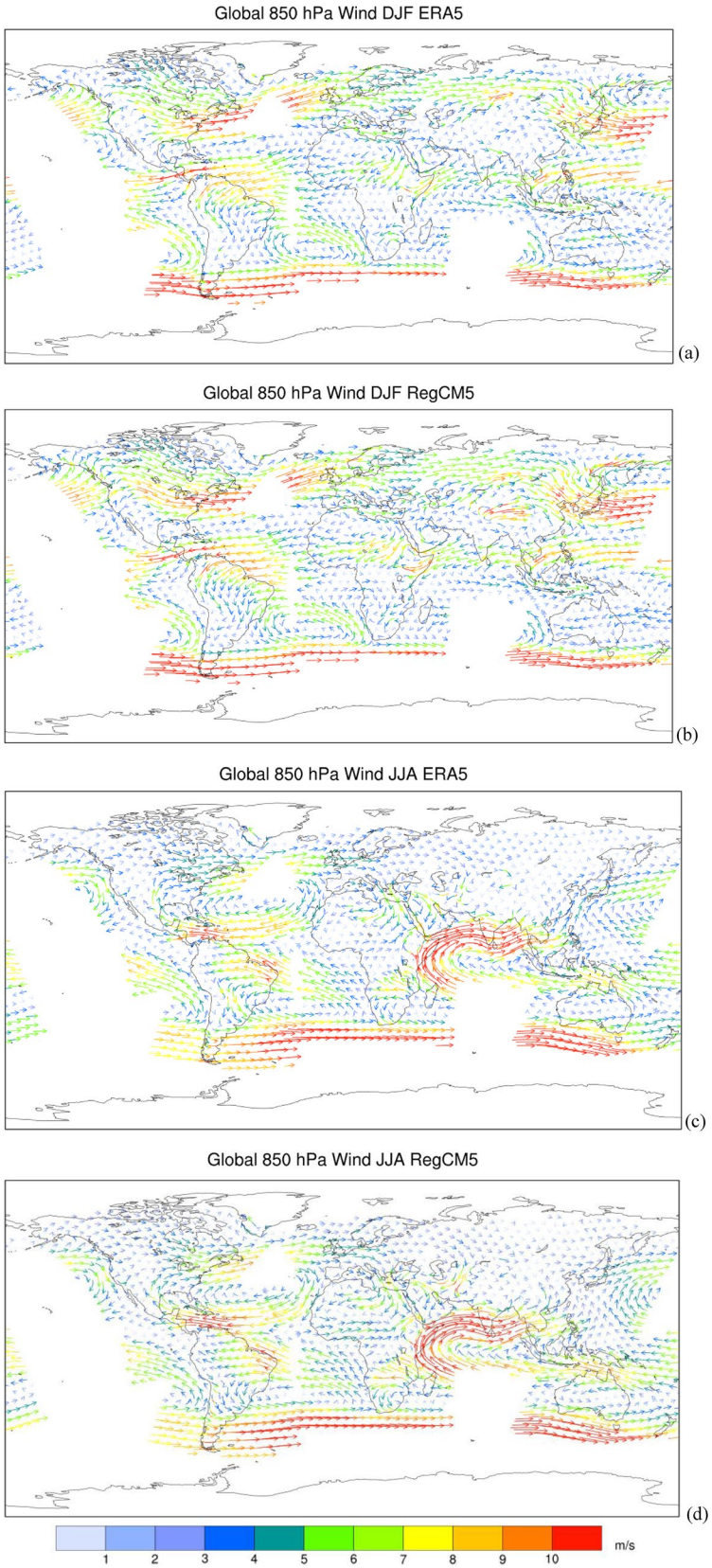

Fig. 4 Wind intensity (m/s) and direction (arrows) at 850 hPa

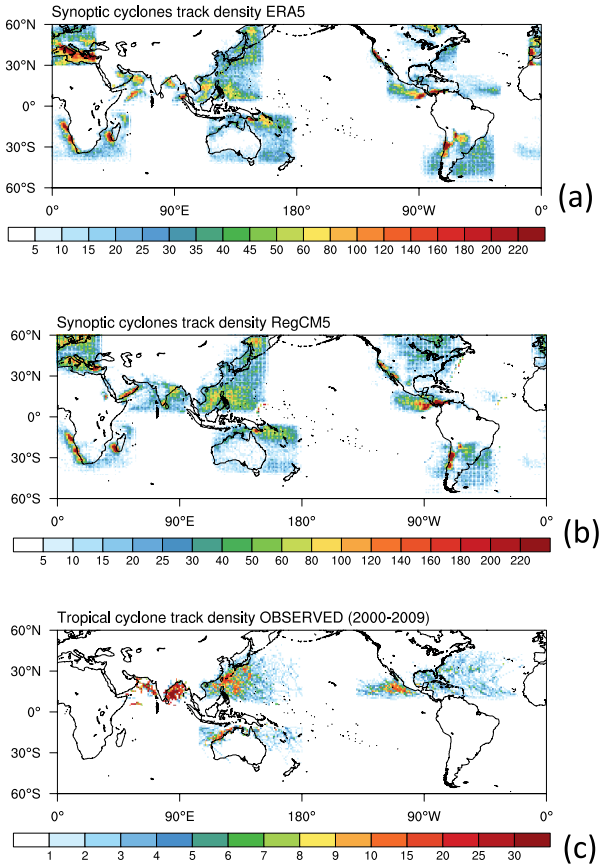

Fig. 5 Total track density of all synoptic cyclones identified in ERA5 (panel a) and RegCM5 (panel b), from 2000 to 2009, using Reboita et al. (2010) algorithm. The unit is the number of cyclones with the center inside a 1 × 1º grid-box; total track density of tropical cyclones identified in the IBTrACS (panel c)

3.6 Upper level circulations

Composites of zonal and meridional wind were computed for 3 different pressure levels, i.e., 850, 500, and 250 hPa. RegCM5 includes a function to perform this task, called sigma2p. This function is first executed to interpolate the wind components from the sigma coordinates to pressure levels. Wind at the selected levels is then extracted, and its seasonal means are calculated over the baseline period. Results of different domains are subsequently interpolated onto the grids of the reference dataset, i.e., ERA5, using distance-weighted average mapping. The composite of global wind is then obtained by directly combining the wind of all domains. In cases where there is an overlap between multiple domains, the average is calculated. For ERA5, wind at the three pressure levels averaged over 2000–2009 is used for all domains except for Europe, where the 1980–2010 average is employed. Wind of the reference dataset is then masked with respect to the RegCM composite to facilitate an intuitive comparison between the two.

3.7 Tropical and extratropical cyclones

Tropical and extratropical cyclones were tracked in each domain, but a graphical representation was created by combining all domains into a single map. Three different algorithms for identifying and tracking tropical cyclones (Reboita et al. 2010; Fuentes-Franco et al. 2014, 2017; Hodges 1994, 1995, 1999) were employed, while one algorithm was used for extratropical systems (Reboita et al. 2010).

All algorithms provide as output the latitude and longitude at each time step of the cyclone's lifecycle and other features such as MSLP, relative vorticity etc., depending on the algorithm. With the tracking information, it is possible to compute the track density, which is the number of cyclones passing by an area of 1º × 1º divided by the area of this box. We compared the RegCM5 performance in reproducing the cyclonic systems against the ERA5 reanalysis when working with the Reboita et al. (2010) algorithm and against the International Best Track Archive for Climate Stewardship (IBTrACS, version v04; Knapp et al. 2010, 2018) for the other algorithms. IBTrACS collects observed tropical cyclone data from 11 agencies around the world covering all major ocean basins and provides 6-h data of tropical cyclones locations.

4 Results

4.1 CORDEX-CORE domains

The mean regional biases for mean, maximum, and minimum temperature, mean precipitation, precipitation frequency and intensity, and precipitation above the 99th percentile are presented in Fig. 1 for all four seasons (DJF, MAM, JJA, and SON) and for each region, as well as for the global average. Mean temperature biases are generally constrained between −2 and 2°, except for the two northernmost regions of the North American continent (NWN and NEN) and the northernmost eastern region of Asia (RFE) in DJF, where a stronger warm bias is evident.

This is likely due to the overestimation of cloud water for low and middle clouds which increases downward infrared radiation (Fig. S2), derived from an excessively stable boundary layer not well reproduced by the Holtslag PBL scheme (see Table 3), as previously noted in Güttler et al.(2014), or Bae et al.(2023); Gao and Giorgi (2017).

The stronger negative biases previously seen in WNA and NCA are much improved as well as in the ARP and SAS regions when compared to the previous model version used in the CORDEX-CORE experiment where the RegCM

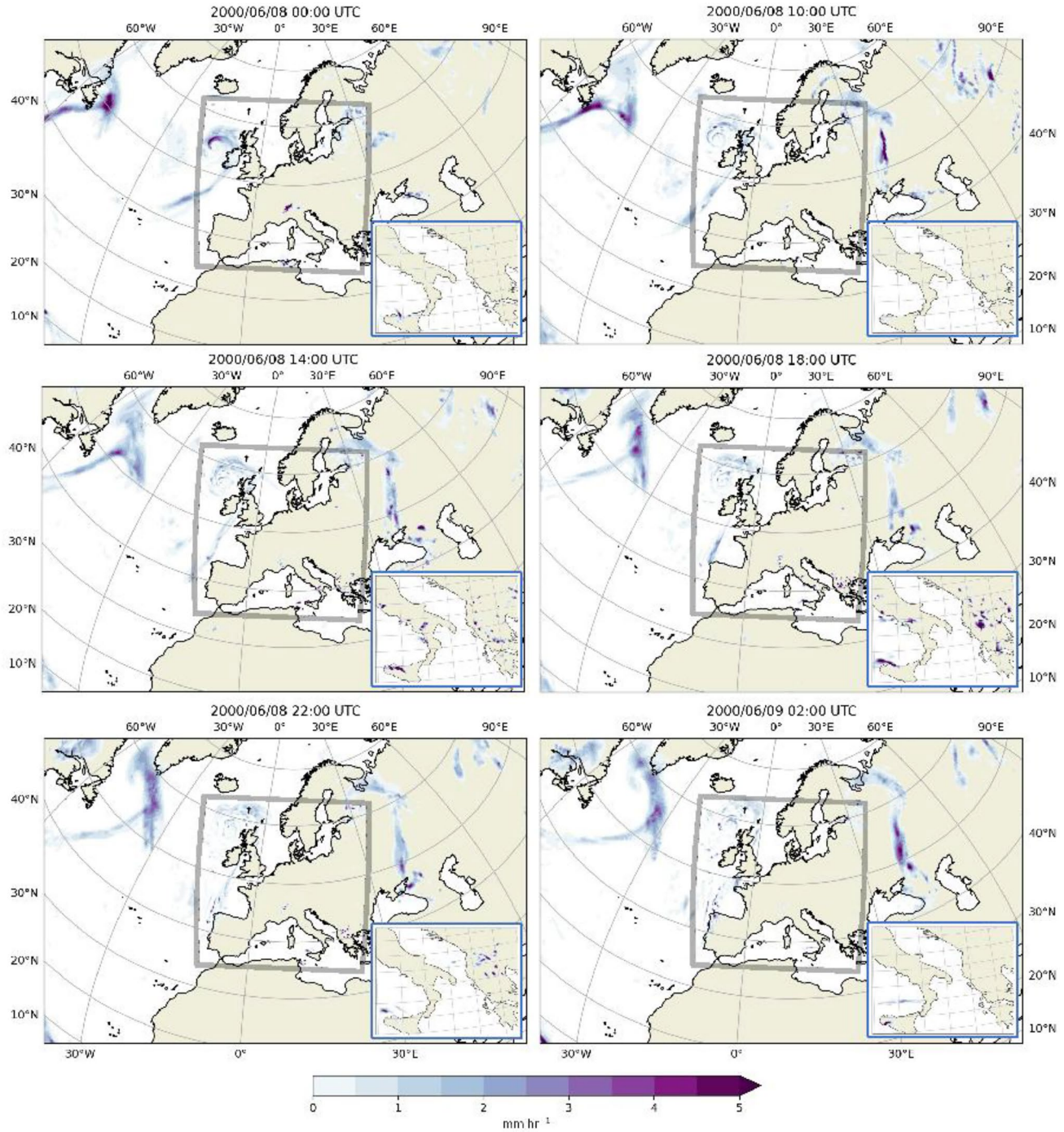

Fig. 6 Precipitation estimates [mm hr^{-1}] from ERA5 and RegCM5 CP for 6 different time steps on the 8th and 9th June 2000. The precipitation estimates inside the gray box are from the RegCM5 CP simulation, while the rest of the domain outside the gray box shows the ERA5 precipitation estimates. The insert figure in each panel shows the RegCM5 CP precipitation estimates over a smaller section of the full domain to highlight the presence of the diurnal cycle in convective activity

model has been driven by three different GCMs (Teichman et al. 2021).

Other outlier regions include central Asia, where the Tibetan Plateau is located, showing a cold bias between 3 and 4 degrees in DJF. This is possibly at least partially due to the well-known sparse nature of available stations at high elevations, especially considering that gauge stations are often placed in valleys and only few or none on mountain tops (Xu et al. 2009) but is well in line with most RCM and GCM biases found in these regions (IPCC Chapter 3

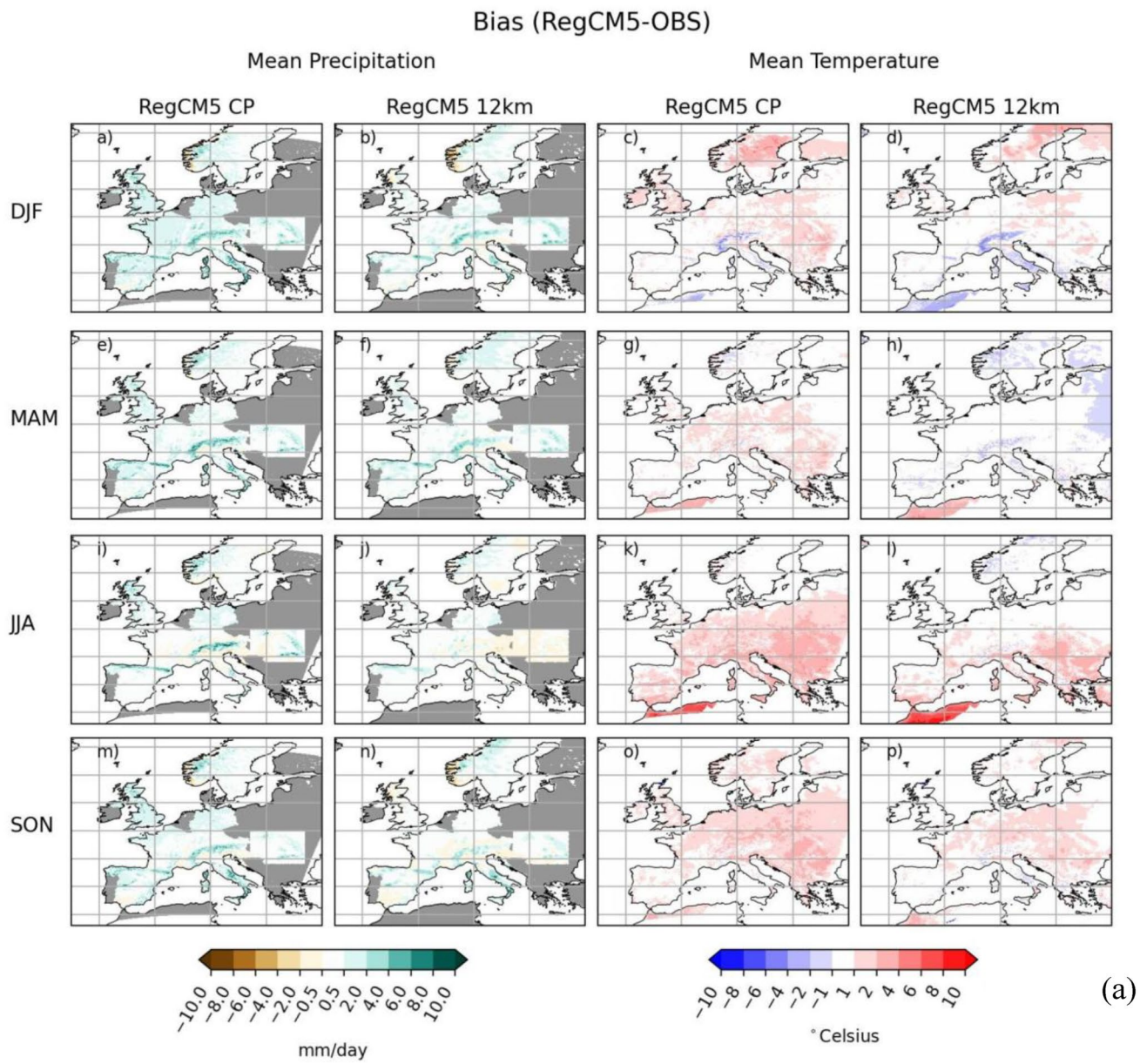

Fig. 7 Mean seasonal bias for Europe CP and Europe 12 km simulation are shown as calculated with respect to the high resolution observation datasets in Table 2. Mean seasonal daily precipitation and mean seasonal temperature are shown in panel a, the seasonal daily precipitation intensity and the precipitation frequency (>1 mm/day) in panel b and the annual P99 bias in panel c. For each variable the left column shows the CP simulation, while the right column represents the results for the Europe 12 km simulations

Fig. 3.3; Eyring et al. 2021). Overall, the model has a tendency for a cold bias in maximum (T_{max}) temperature and a warm bias in minimum (T_{min}) temperature across almost all seasons and regions. This tendency is associated with a systematic overestimation of the lower-level cloud fraction (see Fig. S3), more pronounced in winter than in summer in both hemispheres but consistently present due to an overestimation of cloud liquid water (Fig. S2). In this case, biases are generally within a 2° range, except for the warm T_{min} bias in the Central North-America, Caribbean, western South Africa, and Australasia regions, where the overestimation of the cloud profile is pronounced, and the Tibetan Plateau, showing a cold bias mainly in winter and spring. Cloud ice vertical profiles for DJF and JJA are shown in Fig. S4.

The mean precipitation biases are much improved compared to the previous model version in the South American regions SSA, SWS, SES, NWS and NSA, in North America along the western part of the continent (NCA, WNA, NWN), in North Central-America, in the Sahara and West Southern-Africa and in the Tibetan-Plateau. (Fig. 3 from Teichman et al. 2021) This is consistent with the improvement in the representation in the cloud profiles especially for

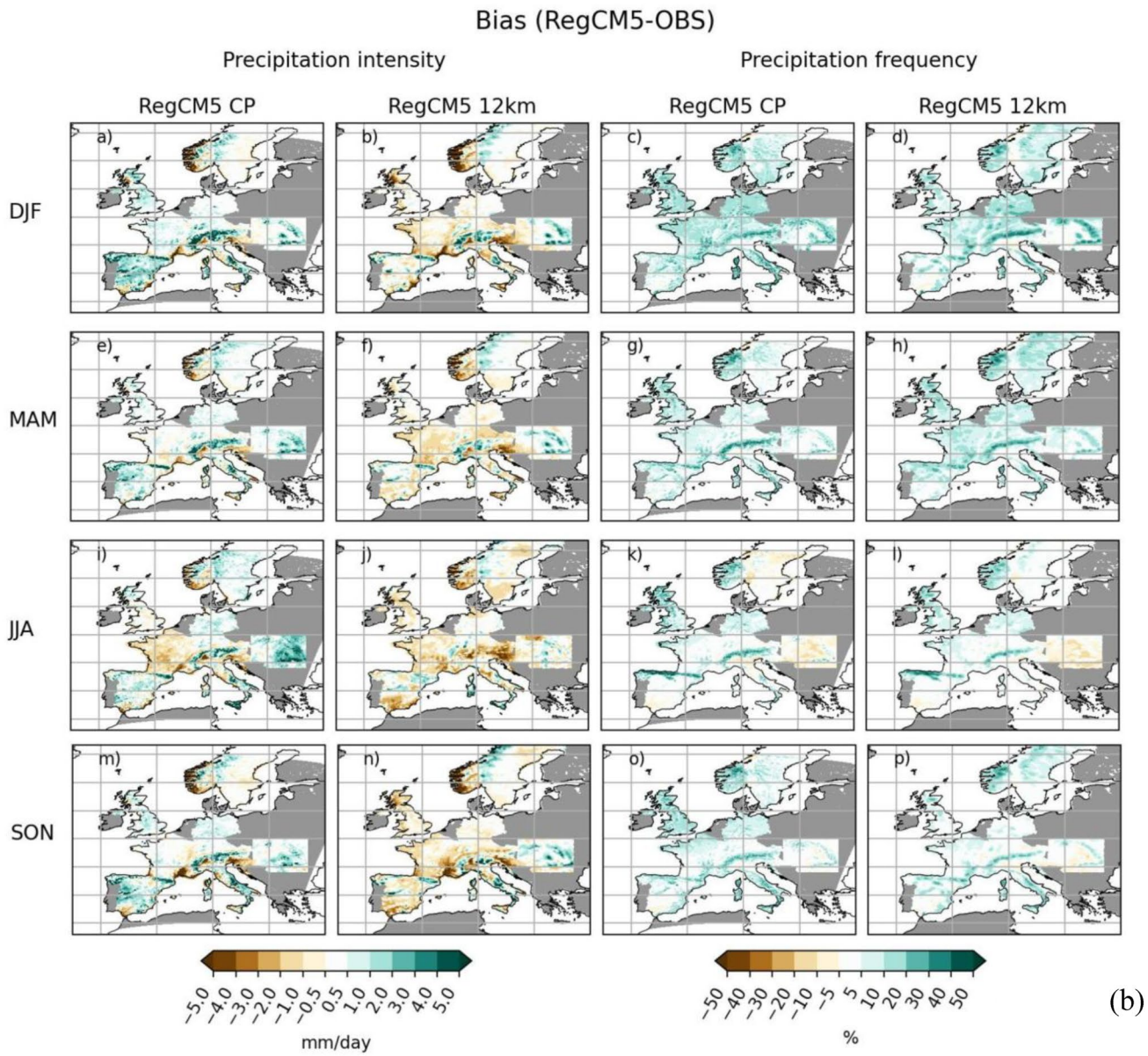

Fig. 7 (continued)

the cloud liquid part (Fig. S2). Compared to the most recent generation of global models (CMIP5 and CMIP6) and high resolution global models (HighResMIP) the RegCM model do not show the typical dry bias over land in the Amazon, La plata basin, India and Indochina, Northern Europe and Western Africa, but rather have a wet bias Over the Andes, Central and Southern Africa and part of Indochina, that are the regions with less data coverage for all the ground based observations (IPCC Chapter 3 Fig. 3.13; Eyring et al. 2021). The intention of these comparisons is not to suggest that model development alone accounts for the improvements, but rather to place our bias results in the broader context of known biases from large ensembles, such as those in CMIP and HighResMIP. In Fig. 2a, Taylor diagrams are presented to validate the spatial temperature patterns in each domain and region, considering only land points. The results show for all seasons a strong correlation (0.9 or higher) between the model and the ERA5 and CRU datasets, except for NSA in South America and the Caribbean region (with respect to CRU), where the correlation drops to 0.7. Similar correlations are observed in Central Africa for all seasons except SON and Western Southern Africa for DJF and MAM. Spatial temperature variability is well captured in all regions, with a tendency to overestimate it in South and Central America (in nearly all regions and seasons) and East Asia, where variability is slightly underestimated for the northernmost regions and overestimated for the southern ones.

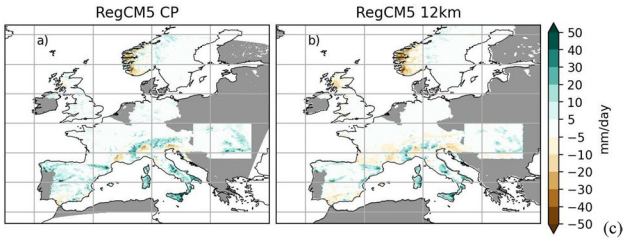

Fig. 7 (continued)

Similar behaviour is observed for maximum and minimum temperature in Figs. S5–S6.

Taylor diagrams for precipitation are presented in Fig. 2b for selected domains and datasets and in Figs. S7 and S8 for the remaining domains and regional observational datasets. Five different datasets are used for comparison, varying in spatial resolution and origin. Correlation and spatial variability for all domains are in better agreement with the MSWEP and GPCC observational products, which have the highest resolution although not prominent in all regions in the same way as in Europe and Central America. Spatial correlation of precipitation ranges between 0.5 and 0.8 in most seasons and regions (Fig. 2b and S7). The model tends to overestimate spatial variability, especially in South America, East Asia, and Africa.

Figure 3 illustrates the comparison of the precipitation intensity distribution in each region between the RegCM5 and RegCM4 models and the observations through box plots. RegCM5 shows a good representation of the precipitation distribution compared to observations and is more realistic than the previous model version, especially for the long tails and most extreme events, where the model strongly ameliorated the problem of numerical grid point storms found in RegCM4. This is quite clear also when compared to the CORDEX-CORE results in the two South America regions SES and NWS, the African regions WAF, SEAF, ESAF, MDG, the South Asia regions SAS and TIB and in the whole South East Asia domain, and it is also evident how the RegCM5 outperforms both CMIP5 and CMIP6 ensemble that show instead a clear underestimation in these regions (Coppola et al. 2021b).

In Fig. 4, the 850 hPa wind field is analyzed to validate monsoon circulation in different continents. The model well represents the South Asia monsoon system in terms of intensity and the wind direction of low-level jet streams. It slightly overestimates the West African monsoon with more inland penetration and a circulation that is too zonal if compared to observations. The Central America and North America monsoons are well located with correct intensity, while the East Asia monsoon circulation intensity is slightly underestimated. The South America Low-Level Jet (SALLJ) is well reproduced in intensity and direction in the austral summer (DJF), while during JJA the jet intensity over south Bolivia and Paraguay is weaker in the model compared to ERA5. The Caribbean Low-Level Jet is well positioned in both seasons with the right intensity and direction. The wind fields at 500 and 200 hPa are also reported in Fig. S9 for completeness.

The model's ability to reproduce the frequency of tropical and extra tropical cyclone tracks was tested using the different tracking algorithms discussed in Methods. As an example of cyclone occurrence, Fig. 5a, b shows cyclone track densities in the RegCM5 simulations and the ERA5 reanalysis calculated with the tracking algorithm of Reboita et al. (2010) and the observed tracks Fig. 5c. The model has a good performance in locating the core of the trajectories in all regions but in some cases with differences in density from ERA5. While there is overestimation over the western Indian Ocean (coastal region of the Arabian Peninsula) and in the extratropical northern European areas and Mediterranean, a slight overestimation occurs in western North America, southern Indian ocean and in the eastern coast of South America. As a comparison in Fig. S10a, b in supplementary material the results of the other two tropical cyclone tracking schemes are reported. Both are also able to reproduce the areas of maximum track density but exhibit different numbers of cyclones in the western tropical Atlantic Ocean, equatorial Indian Ocean region, and eastern Asia tropical Pacific Ocean.

These results highlight the importance of the choice of the tracking algorithm and the associated uncertainty in model results due to the specific algorithm that is used.

4.2 Pan European CP domain

As mentioned, by being much more computationally efficient than previous versions of the model, RegCM5 allows simulations for a pan-European domain at convection-permitting resolution. Figure 6 illustrates a time sequence of summer convective events in the southern regions of Italy and Greece within the 3 km CP domain, which is outlined by the grey square, while ERA5 precipitation is shown outside of this region. The sequence aims at showing how the model is able to initiate convection at such resolution within the gray box. It starts on the night of June 8, 2000. A storm enters the CP domain from the western boundary, crossing Ireland throughout the day. Convection initiates in Sicily, Calabria, and northern Greece in the early afternoon, reaching its peak at 18:00 UTC and diminishing later in the evening. The time lapse demonstrates the consistency between the ERA5 boundary conditions and the CP model simulation in the evolution of the storm event as expected and the

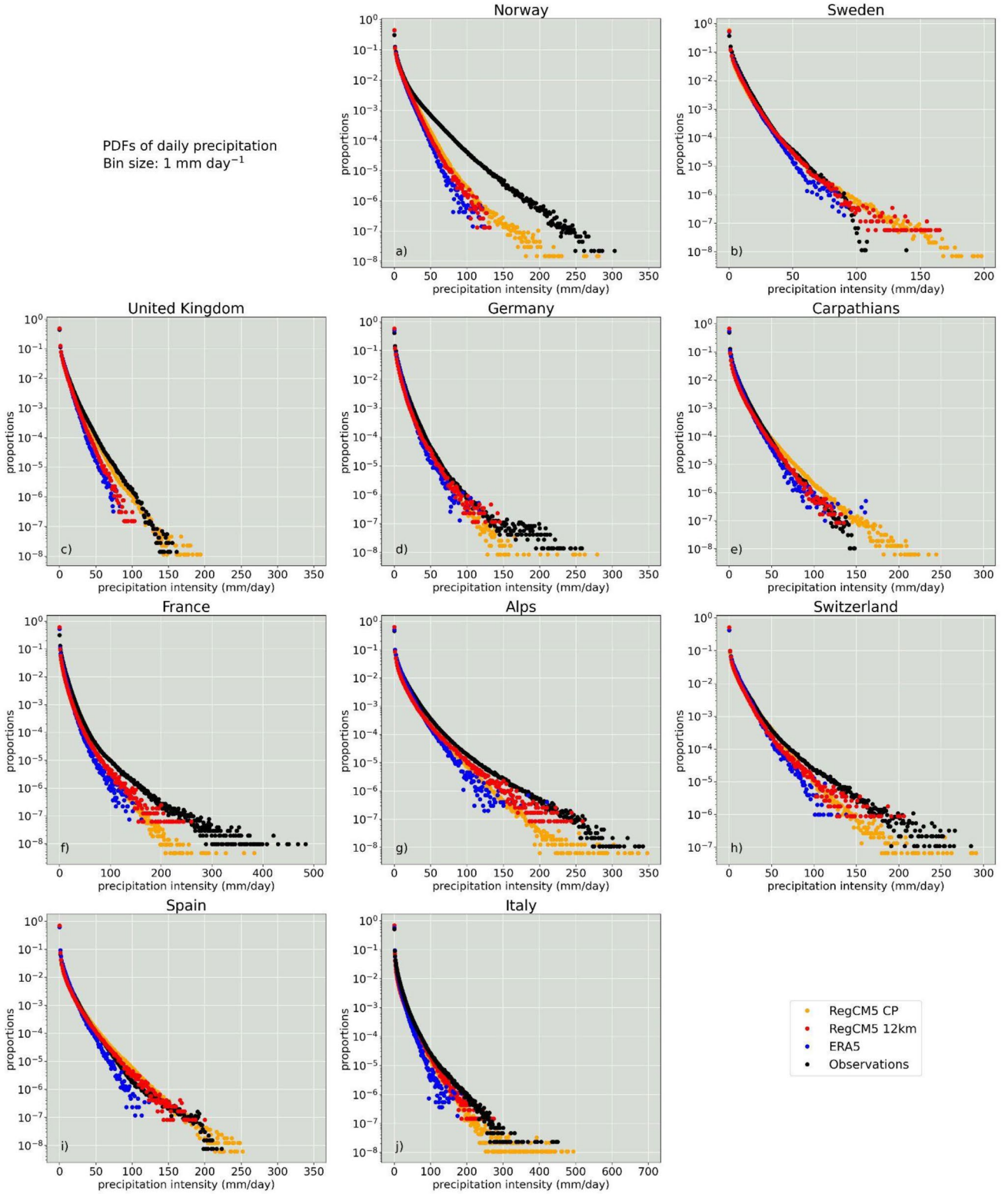

Fig. 8 Probability density function distributions of the daily precipitation [mm day^{-1}] for the 10 regions investigated in the European domain. Each panel shows the distribution estimated from combining all available data in each domain for the years 2000–2009 for RegCM5 CP (orange), RegCM5 12 km (red), ERA5 (blue) and observations (black). Details about the observational datasets for each region can be found in Table 2

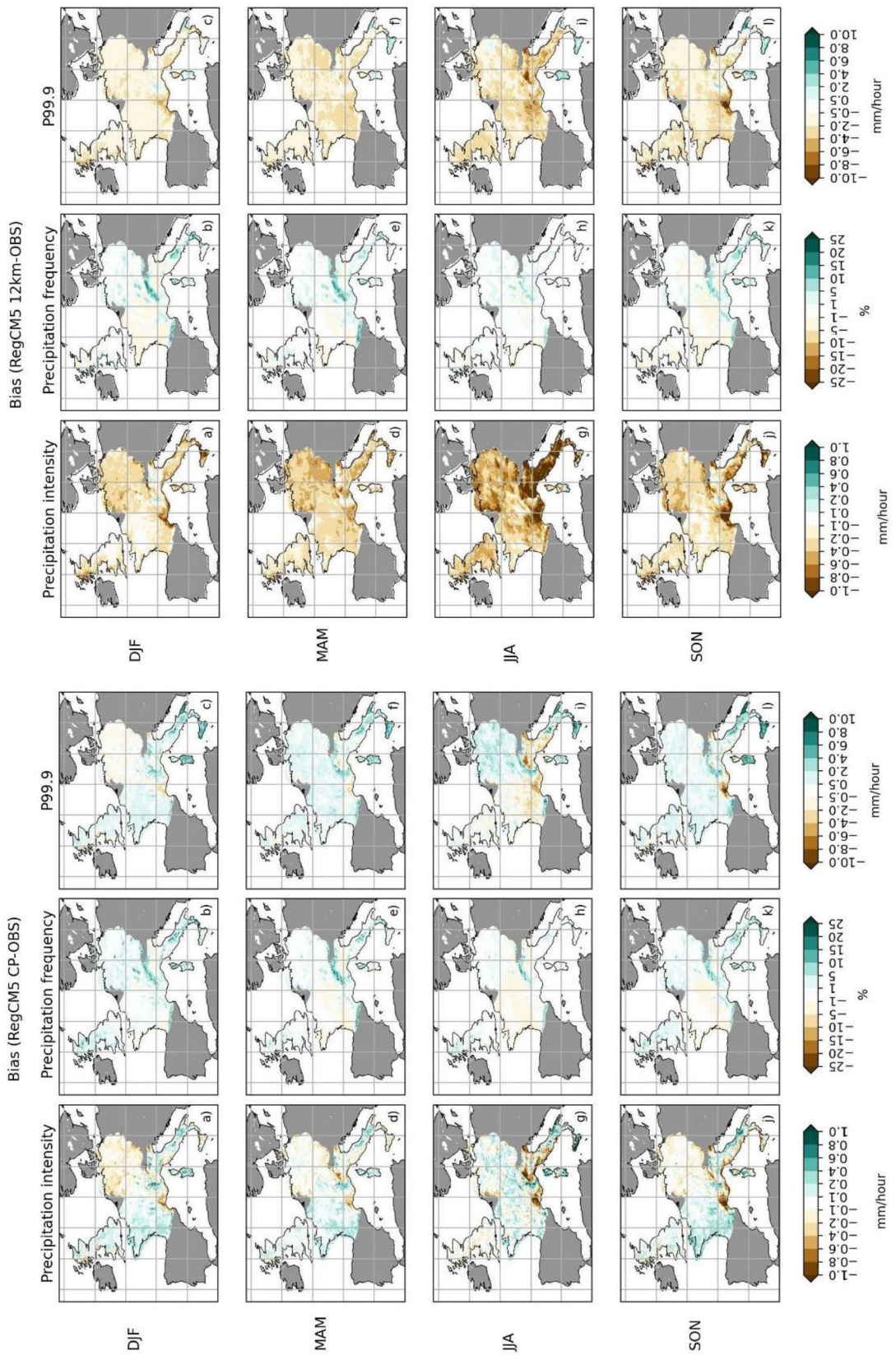

Fig. 9 Precipitation intensity, wet frequency and P99.9 seasonal bias for hourly RegCM5 CP (panel a) and RegCM5 12 km (panel b) versus high resolution observations. In each panel, the first column shows the seasonal biases for precipitation intensity, second column the precipitation frequency bias and the third column the P99.9 bias. The threshold used as the minimum precipitation for the RegCM5 simulations is 0.5 mm/hr. Figure S12 (panels a and b) shows the same seasonal biases but using the minimum threshold of 0.1 mm/hr

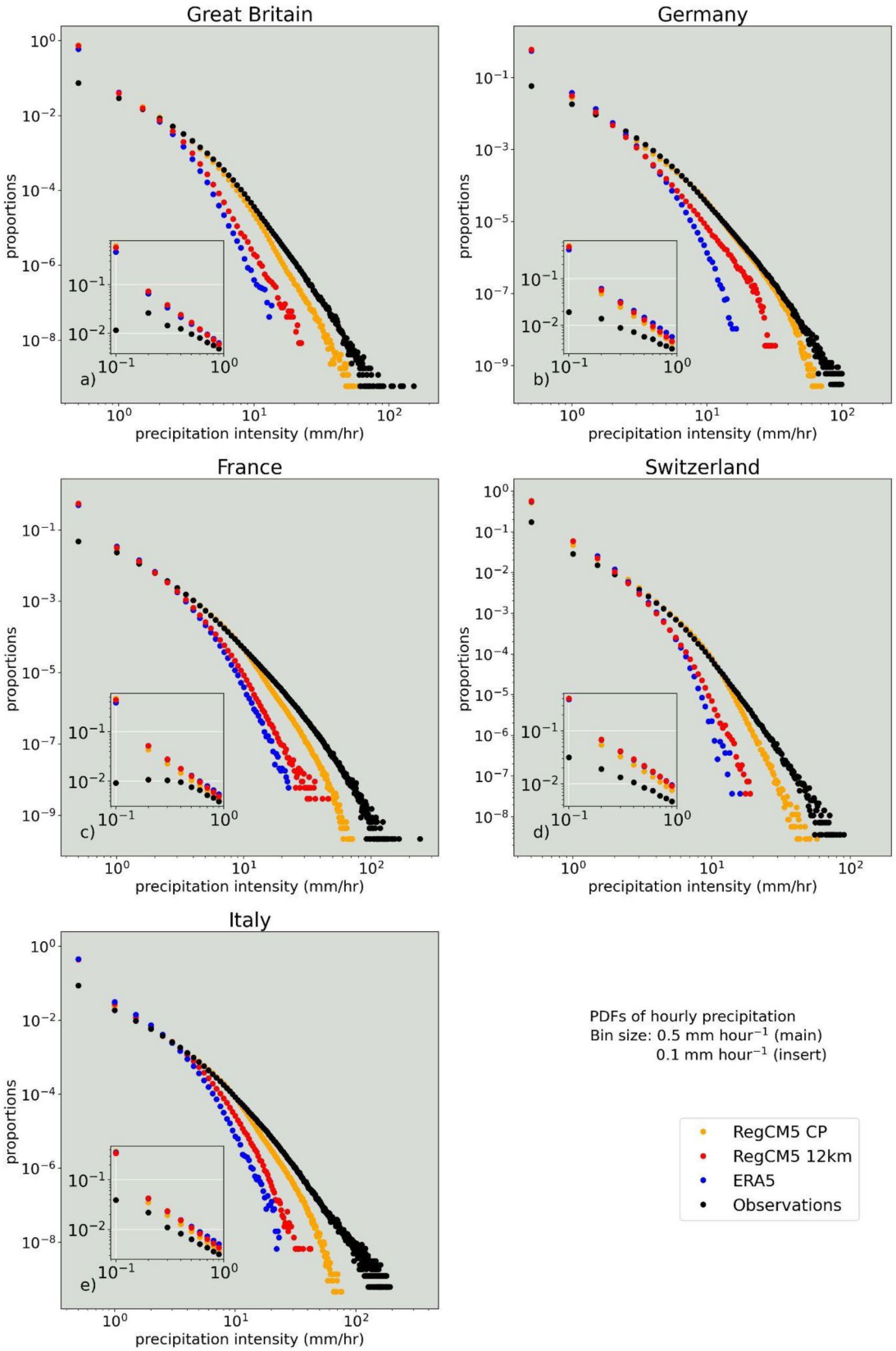
Great Britain
Germany
France
Switzerland
Italy
proportions
precipitation intensity (mm/hr)
a)
b)
c)
d)
e)
PDFs of hourly precipitation
Bin size: 0.5 mm hour^{-1} (main)
0.1 mm hour^{-1} (insert)
RegCM5 CP
RegCM5 12km
ERA5
Observations

Fig. 10 PDFs of hourly precipitation for the RegCM5 Convection Permitting simulation (orange), the RegCM5 12 km simulation (red), ERA5 (blue) and high resolution observations (black) from 5 regions (Great Britain, Germany, France, Switzerland and Italy). Each figure represents the distribution based on all the data available over the domain and time interval investigated. The bin size resolution is 0.5 mm/hr. The insert figure in each panel shows a breakdown of the three lowest precipitation intensity bins in the main panel, using a bin size resolution of 0.1 mm/hr

RegCM5 model ability to trigger summer convection when km-scale resolution is reached.

Figure 7 shows seasonal precipitation and temperature biases, precipitation frequency and intensity, and p99 biases for the convection-parametrized 12 km resolution run and the explicit convection 3 km resolution run (CP). Table 2 presents the observed datasets used for model validation, which are station-based or radar-based national datasets for various European countries (the highest resolution ones are used as a benchmark for the CP validation). Both resolutions exhibit similar mean temperature and precipitation biases, mean daily precipitation frequency and P99 biases, while improvements in daily precipitation intensity bias at the 3 km resolution (CP) are found widespread in many regions and all seasons.

Comparing RegCM5 CP simulation with CORDEX-FPSCONV (Coppola et al. 2020) CP ensemble in Ban et al. (2021, their Fig. 8) over common areas in Switzerland (CH), France (FR) and Italy (IT) within their Great Alpine region (their Fig. 1), we find the pan-European CP simulation laying within their model spread of percentage biases close to the median value or even with a lower absolute value compared to the ensemble distribution for mean daily precipitation, intensity and frequency.

Figure 8 compares precipitation probability density function distributions at a daily timescale for each observed dataset. The CP precipitation distribution aligns closely with the high-resolution datasets, outperforming the 12 km resolution model and ERA5 precipitation distribution in most regions. However, in Norway, the CP model distribution underestimates the observed one probably due to the quite high 1 km resolution (Mohr et al. 2009) of the dataset and the very complex topography that creates a misalignment between the station and the model gridpoint location, and in the Carpathians and Spain regions, the model overestimates the precipitation distribution, possibly due to the lower resolution of station-based observations (Fantini et al. 2018). An underestimation is also seen in Germany and France for the tail of the distribution that is probably connected with the underestimation of the daily intensity in southern France and Germany (see Fig. 7b).

Supplementary Fig. S11 illustrates daily temperature PDFs for the same regions, showing reasonable temperature distributions with a slight underestimation of maximum temperature values in areas of complex topography, such as the Alps and Swiss regions, likely attributed to a precipitation overestimation.

Figures 9, 10, and 11 present precipitation statistics at hourly timescale. Frequency, intensity, and very extreme hourly precipitation (p99.9) are computed for events above the threshold of 0.5 mm/h, revealing a tendency for orographically driven positive bias for CP resolution mainly evident in frequency. Despite some regional discrepancies, the explicit representation of convection in the CP run reduces systematic biases compared to the 12 km simulation across all statistics and seasons. Supplementary Fig. S12a, b show results with a more commonly used threshold of 0.1 mm/h, indicating a noticeable negative and positive bias for intensity and frequency, respectively, in the 3 km resolution (CP), primarily attributed to very light events occurring between 0.1 and 0.5 mm/h. This is also evident in Fig. 10, where the hourly precipitation distributions are reported for five regions. The high resolution model precipitation matches well with the observed distribution, with a noteworthy mismatch occurring in the range 0.1–0.5 mm/h for all the model resolutions and the ERA5 precipitation distributions. The low resolution models systematically underestimate precipitation values larger than 15 mm/h in almost all regions, while the CP simulation reduces the gap with observed values.

Compared with CORDEX-FPSCONV CP ensemble (Fig. 8 of Ban et al. 2021), the hourly frequency bias is systematically lower than the median ensemble value, whereas the intensity bias is on the lower edge of the ensemble distribution and outlier in the spring season and sometimes in the winter season.

Finally, Fig. 11 shows the diurnal cycle of five precipitation statistics for the same five regions as in Fig. 10 and the JJA season. The explicit representation of convection better reproduces both the phase and amplitude of the diurnal cycle in most statistics and regions if compared with the coarser resolution model. It is worth noticing the strange behaviour of the observed dataset in Great Britain due to the way they fill the missing data for the 11 UTC (Lewis et al. 2018) and the position of the CP model maximum for mean precipitation shifted to the late hours of the day as well as the flat frequency curve for both Germany and France that is also found in the CORDEX-FPSCONV CP ensemble (Fig. 11 of Ban et al. 2021). This is probably due to the greater latitudinal extension of the Germany and France domains: averaging spatially over large areas that can be characterized by different diurnal cycle of convection, can lead to a further difficulty for the models to represent this gradient, as shown already by Berthou et al. (2020). The daily cycles for DJF, SON and MAM are reported in Fig. S13 for completeness.

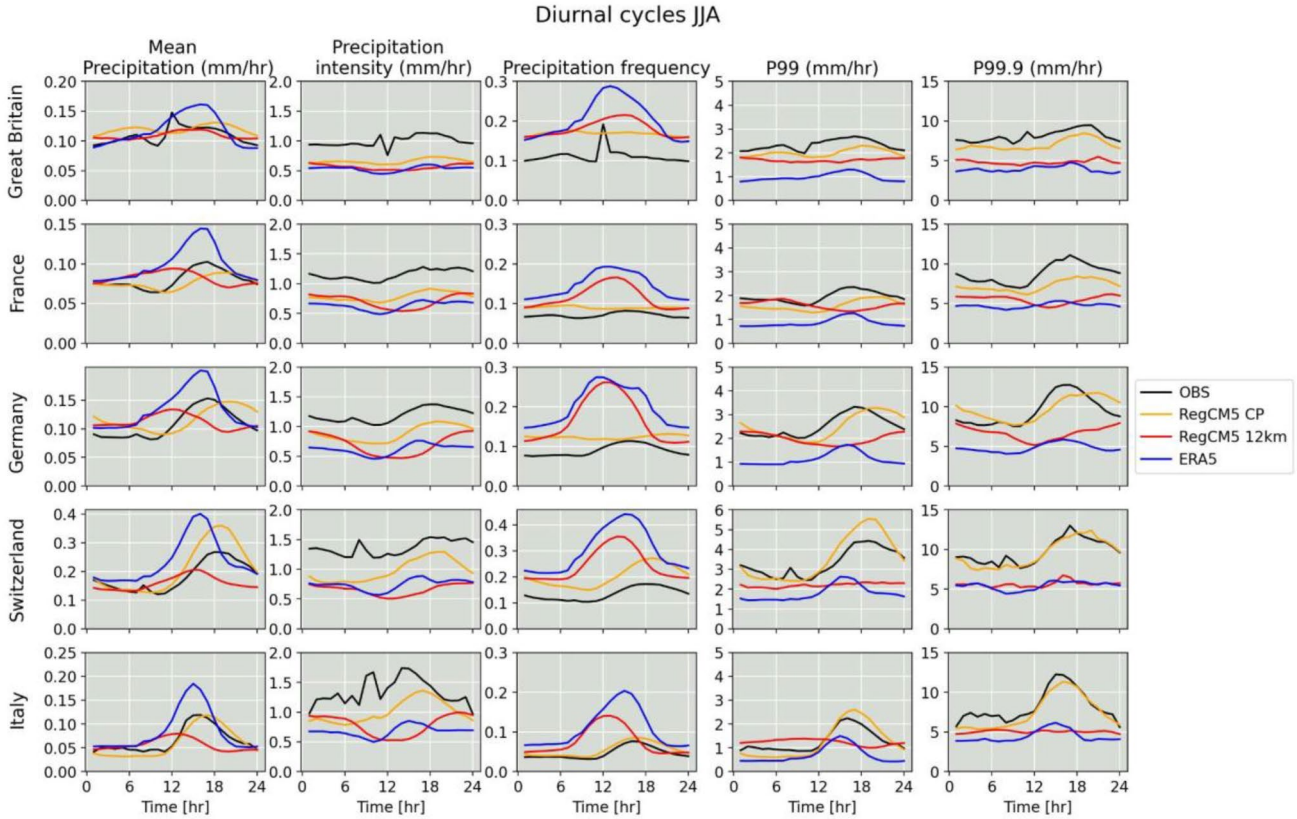

Fig. 11 Diurnal cycles for mean precipitation (first column), precipitation intensity (second column), precipitation frequency (third column), p99 (fourth column) and p99.9 (fifth column) in JJA for 5 regions in Europe: Great Britain (top row), France (second row), Germany (third row), Switzerland (fourth row) and Italy (bottom row). The same figures for DJF, SON and MAM are shown in the Supplementary material

5 Summary and outlook

The Regional Climate Modeling system (RegCM) has evolved significantly since its inception, with versions such as RegCM4 and RegCM4-NH playing pivotal roles in climate research and participating in international projects such as CORDEX. These models, however, require relatively small time steps, and thus present limitations especially when applied at CP resolutions. The recently developed RegCM5 incorporates the dynamical core from the non-hydrostatic weather prediction model MOLOCH's to enhance the computational efficiency and stability of the model. This paper aims to comprehensively evaluate the performance of RegCM5, focusing on convection-parametrized and convection-permitting scales across various CORDEX-CORE domains, and including for the first time a pan-European domain at convection-permitting resolution. The assessment encompasses temperature biases, precipitation patterns, monsoon circulations, extratropical and tropical cyclone tracks, and the model's ability to explicitly simulate convective events.

The evaluation of RegCM5 shows important improvements in addressing challenges posed by smaller scale processes, offering improved capabilities for understanding climate dynamics and projections. The model demonstrates good performance in capturing temperature patterns, precipitation distributions, and monsoon circulations across various regions and improvements compared to the previous model version RegCM4 used for the CORDEX-CORE experiment and the CORDEX-FPSCONV. The implementation of RegCM5's pan-European convection-permitting domain offers enhanced representation of daily and hourly precipitation patterns, as well as the diurnal cycle, compared to the convection-parametrized model version. It also demonstrates the feasibility of running at such high spatial resolutions over larger domains on climatological time scales.

The model is currently available for use by the RegCM community and other prospective users. In this paper we have used for the different domains, model configurations that can be adopted as starting points for optimizing the model performance for different applications. Being a new development, the model needs to be further tested, and in this regard the contribution and feedback from the broader model community are essential. We are currently further improving the model capabilities, for example updating the land surface scheme CLM, the PBL scheme and including

a two moment 6 hydrometeors microphysical scheme, and fine tuning some of the model's available physics options. We are also planning to develop a model version usable on GPU-based computing architectures. We expect that RegCM5 will be the leading model version used by the RegCM community and maintained by the ICTP development team over the next several years.

Supplementary Information The online version contains supplementary material available at https://doi.org/10.1007/s00382-025-07913-3.

Funding The study was not funded by any specific grant, research program or institutional support.

Data availability The RegCM5 model code is available at: https://doi.org/10.5281/zenodo.17348622. The ERA5 data used in this work can be found at: https://doi.org/10.24381/cds.bd0915c6. The model is distributed with a public licence and available for download from the github repository: https://github.com/ICTP/RegCM. Data and scripts for the analysis are available at https://github.com/graziano-giuliani/RegCM5_CORDEX_prepare.

Declarations

Conflict of interest There is no conflict of interest in any element of the manuscript.

Ethical approval The article does not contain any studies involving human or animal participants.

References

Anthes RA, Hsie EY, Kuo YH (1987) Description of the Penn State/NCAR mesoscale model version 4 (MM4). National Center for Atmospheric Research Tech Note TN-282+STR, NCAR, Boulder, CO

Artale V, Calmanti S, Carillo A, Dell'Aquila A et al (2010) An atmosphere–ocean regional climate model for the Mediterranean area: assessment of a present climate simulation. Clim Dyn 35:721–740

Bae J, Sung H-J, Baek E-H, Choi J-H, Lee H-J, Kim B-M (2023) Reduction in the Arctic Surface Warm Bias in the NCAR CAM6 by reducing excessive low-level clouds in the Arctic. Atmosphere 14:522. https://doi.org/10.3390/atmos14030522

Ban N, Caillaud C, Coppola E, Pichelli E, Sobolowski S, Adinolfi M et al (2021) The first multi-model ensemble of regional climate simulations at kilometer-scale resolution part 1: evaluation of precipitation. Clim Dyn 57(1–2):275–302. https://doi.org/10.1007/s00382-021-05708-w

Beck HE, Pan M, Roy T, Weedon GP, Pappenberger F, van Dijk AIJM, Huffman GJ, Adler RF, Wood EF (2019) Daily evaluation of 26 precipitation datasets using Stage-IV gauge-radar data for the CONUS. Hydrol Earth Syst Sci 23:207–224. https://doi.org/10.5194/hess-23-207-2019

Berthou S, Kendon EJ, Chan SC, Ban N, Leutwyler D, Schär C, Fosser G (2020) Pan-European climate at convection-permitting scale: a model intercomparison study. Clim Dyn 55:35–59

Bettolli M, Solman S, da Rocha R et al (2021) The CORDEX flagship pilot study in southeastern South America: a comparative study of statistical and dynamical downscaling models in simulating daily extreme precipitation events. Clim Dyn 56(5):1589–1608

Bretherton CS, McCaa JR, Grenier H (2004) A new parameterization for shallow cumulus convection and its application to marine subtropical cloud-topped boundary layers. I. Description and 1D results. Mon Weather Rev 132:864–882

Buzzi A, Davolio S, Malguzzi P, Drofa O, Mastrangelo D (2014) Heavy rain episodes over Liguria in autumn 2011: numerical forecasting experiments. Nat Hazards Earth Syst Sci 14(5):1325–1340. https://doi.org/10.5194/nhess-14-1325-2014

Chen M, Shi W, Xie P, Silva VBS, Kousky VE, Higgins RW, Janowiak JE (2008) Assessing objective techniques for gauge-based analyses of global daily precipitation. J Geophys Res Atmos 113:D04110. https://doi.org/10.1029/2007jd009132

Coppola E, Giorgi F, Mariotti L, Bi X (2012) RegT-Band: a tropical band version of RegCM4. Clim Res 52:115–133. https://doi.org/10.3354/cr01078

Coppola E, Sobolowski S, Pichelli E et al (2020) A first-of-its-kind multi-model convection permitting ensemble for investigating convective phenomena over Europe and the Mediterranean. Clim Dyn 55:3–34. https://doi.org/10.1007/s00382-018-4521-8

Coppola E, Stocchi P, Pichelli E, Torres Alavez JA, Glazer R, Giuliani G, Di Sante F, Nogherotto R, Giorgi F (2021a) Non-hydrostatic RegCM4 (RegCM4-NH): model description and case studies over multiple domains. Geosci Model Dev 14:7705–7723. https://doi.org/10.5194/gmd-14-7705-2021

Coppola E, Raffaele F, Giorgi F et al (2021b) Climate hazard indices projections based on CORDEX-CORE, CMIP5 and CMIP6 ensemble. Clim Dyn 57:1293–1383. https://doi.org/10.1007/s00382-021-05640-z

Cornes R, van der Schrier G, van den Besselaar EJM, Jones PD (2018) An ensemble version of the E-OBS temperature and precipitation datasets. J Geophys Res Atmos. https://doi.org/10.1029/2017JD028200

da Rocha RP, Llopart M, Reboita MS, Bettolli ML, Solman S, Fernández J, Milovac J, Feijoó M, Coppola E (2024) Precipitation diurnal cycle assessment in convection-permitting simulations in Southeastern South America. Earth Syst Environ 8(1):1–19

Davolio S, Malguzzi P, Drofa O, Mastrangelo D, Buzzi A (2020) The Piedmont flood of November 1994: a test-bed of forecasting capabilities of the CNR-ISAC meteorological model suite. Bull Atmos Sci Technol 1:263–282

Dickinson RE, Errico RM, Giorgi F, Bates GT (1989) A regional climate model for the western United States. Clim Change 15(3):383–422. https://doi.org/10.1007/BF00240465

Dickinson RE, Henderson-Sellers A, Kennedy PJ (1993) Biosphere-atmosphere transfer scheme (BATS) version 1e as coupled to the NCAR community climate model (No. NCAR/TN-387+STR). University Corporation for Atmospheric Research. https://doi.org/10.5065/D67W6959

Di Sante F, Coppola E, Farneti R, Giorgi F (2019) Indian summer monsoon as simulated by the regional earth system model RegCM-ES: the role of local air–sea interaction. Clim Dyn 53:759–778

Emanuel KA, Zivkovic-Rothman M (1999) Development and evaluation of a convection scheme for use in climate models. J Atmos Sci 56:1766–1782

Eyring V, Gillett NP, Achuta Rao KM, Barimalala R, Barreiro Parrillo M, Bellouin N, Cassou C, Durack PJ, Kosaka Y, McGregor S, Min S, Morgenstern O, Sun Y (2021) Human influence on the climate system. In: Masson-Delmotte V, Zhai P, Pirani A, Connors SL, Péan C, Berger S, Caud N, Chen Y, Goldfarb L, Gomis MI, Huang M, Leitzell K, Lonnoy E, Matthews JBR, Maycock TK, Waterfield T, Yelekçi O, Yu R, Zhou B (eds) Climate change 2021: the physical science basis contribution of working group I to the 6th assessment report of the intergovernmental panel on climate change. Cambridge University Press, Cambridge, pp 423–552. https://doi.org/10.1017/9781009157896.005

Fairall CW, Bradley EF, Hare JE, Grachev AA, Edson JB (2003) Bulk parameterization of air-sea fluxes: updates and verification for the COARE algorithm. J Climate 16:571–591

Fantini A, Raffaele F, Torma C et al (2018) Assessment of multiple daily precipitation statistics in ERA-Interim driven Med-CORDEX and EURO-CORDEX experiments against high resolution observations. Clim Dyn 51:877–900. https://doi.org/10.1007/s00382-016-3453-4

Fantini A (2019) Climate change impact on flood hazard over Italy. University of Trieste, Trieste

Fuentes-Franco R, Coppola E, Giorgi F et al (2014) Assessment of RegCM4 simulated inter-annual variability and daily-scale statistics of temperature and precipitation over Mexico. Clim Dyn 42:629–647. https://doi.org/10.1007/s00382-013-1686-z

Fuentes-Franco R, Giorgi F, Coppola E et al (2017) Sensitivity of tropical cyclones to resolution, convection scheme and ocean flux parameterization over Eastern tropical Pacific and tropical North Atlantic oceans in the RegCM4 model. Clim Dyn 49:547–561. https://doi.org/10.1007/s00382-016-3357-3

Gao XJ, Giorgi F (2017) Use of the RegCM system over East Asia: review and perspectives. Engineering 3(5):766–772

Gelaro R, McCarty W, Suarez MJ, Todling R, Molod A, Takacs L, Randles CA, Darmenov A, Bosilovich MG, Reichle R, Wargan K, Coy L, Cullather R, Draper C, Akella S, Buchard V, Conaty A, da Silva AM, Gu W, Kim G-K, Koster R, Lucchesi R, Merkova D, Nielsen JE, Partyka G, Pawson S, Putman W, Rienecker M, Schubert SD, Sienkiewicz M, Zhao B (2017) The modern-era retrospective analysis for research and applications, version 2 (MERRA-2). J Climate 30(14):5419–5454. https://doi.org/10.1175/JCLI-D-16-0758.1

Giorgi F, Bates GT (1989) The climatological skill of a regional model over complex terrain. Mon Weather Rev 117(11):2325–2347

Giorgi F, Marinucci MR, Bates GT (1993a) Development of a second generation regional climate model (RegCM2). Part I: boundary layer and radiative transfer processes. Mon Weather Rev 121(10):2794–2813

Giorgi F, Marinucci MR, Bates GT, De Canio G (1993b) Development of a second-generation regional climate model (RegCM2). Part II: convective processes and assimilation of lateral boundary conditions. Mon Weather Rev 121(10):2814–2832

Giorgi F, Mearns LO (1999) Introduction to special section: regional climate modeling revisited. J Geophys Res 104(D6):6335–6352. https://doi.org/10.1029/98jd02072

Giorgi F, Francisco R, Pal JS (2003) Effects of a sub-grid scale topography and landuse scheme on surface climate and hydrology. I. Effects of temperature and water vapor disaggregation. J Hydrometeorol 4:317–333

Giorgi F, Jones C, Asrar G (2009) Addressing climate information needs at the regional level: the CORDEX framework. World Meteorol Organ Bull 58:175–183

Giorgi F, Coppola E, Solmon F, Mariotti L, Sylla M, Bi X et al (2012) RegCM4: model description and preliminary tests over multiple CORDEX domains. Clim Res 52:31–48. https://doi.org/10.3354/cr01018

Giorgi F, Coppola E, Jacob D, Teichmann C, Abba Omar S, Ashfaq M, Ban N, Bülow K, Bukovsky M, Buntemeyer L, Cavazos T, Ciarlo` J, da Rocha RP, Das S, di Sante F, Evans JP, Gao X, Giuliani G, Glazer RH, Hoffmann P, Im E-S, Langendijk G, Lierhammer L, Llopart M, Mueller S, Luna-Nino R, Nogherotto R, Pichelli E, Raffaele F, Reboita M, Rechid D, Remedio A, Remke T, Sawadogo W, Sieck K, Torres-Alavez JA, Weber T (2022) The CORDEX- CORE EXP-I initiative: description and highlight results from the initial analysis. Bull Am Meteorol Soc 103(2):E293–E310

Giorgi F, Coppola E, Giuliani G, Ciarlò JM, Pichelli E, Nogherotto R, Raffaele F, Malguzzi P, Davolio S, Stocchi P, Drofa O (2023a) The fifth generation regional climate modeling system, RegCM5: description and illustrative examples at parameterized convection and convection-permitting resolutions. J Geophys Res Atmos 128(6):38199. https://doi.org/10.1029/2022JD038199

Giorgi F, Coppola E, Giuliani G, Ciarlò JM, Pichelli E, Nogherotto R, Raffaele F, Malguzzi P, Davolio S, Stocchi P, Drofa O (2023b) RegCM-NH V5 code: January 18, 2023 release (Version 5.0.0) [Software]. Zenodo. https://doi.org/10.5281/zenodo.7548172

Grell GA (1993) Prognostic evaluation of assumptions used by cumulus parameterizations. Mon Weather Rev 121:764–787. https://doi.org/10.1175/1520-0493(1993)121%3c0764:PEOAUB%3e2.0.CO;2

Grell G, Dudhia J, Stauffer DR (1994) A description of the fifth generation Penn State/NCAR mesoscale model (MM5). NCAR technical note NCAR/TN-398 + STR, pp 121

Güttler I, Branković Č, O'Brien TA et al (2014) Sensitivity of the regional climate model RegCM4.2 to planetary boundary layer parameterisation. Clim Dyn 43:1753–1772. https://doi.org/10.1007/s00382-013-2003-6

Gutowski WJ, Giorgi F, Timbal B, Frigon A, Jacob D, Kang H-S et al (2016) WCRP coordinated regional downscaling experiment (CORDEX): a diagnostic MIP to CMIP6. Geosc Model Dev 9:4087–4095

Harris I, Osborn TJ, Jones P, Lister D (2020) Version 4 of the CRU TS monthly high-resolution gridded multivariate climate dataset. Sci Data 7(1):109. https://doi.org/10.1038/s41597-020-0453-3

Herrera S, Gutiérrez JM, Ancell R, Pons MR, Frías MD, Fernández J (2010) Development and analysis of a 50-year high-resolution daily gridded precipitation dataset over Spain (Spain02). Int J Climatol 32(1):74–85

Hersbach H, Bell B, Berrisford P, Hirahara S, Horányi A, Muñoz-Sabater J, Thépaut JN (2020) The ERA5 global reanalysis. Q J R Meteorol Soc 146:1999–2049. https://doi.org/10.1002/qj.3803

Hersbach H, Bell B, Berrisford P, Biavati G, Horányi A, Muñoz Sabater J, Nicolas J, Peubey C, Radu R, Rozum I, Schepers D, Simmons A, Soci C, Dee D, Thépaut J-N (2023) ERA5 hourly data on pressure levels from 1940 to present. Copernicus Climate Change Service (C3S) Climate Data Store (CDS). https://doi.org/10.24381/cds.bd0915c6

Hodges KI (1994) A general-method for tracking analysis and its application to meteorological data. Mon Weather Rev 122(11):2573–2586. https://doi.org/10.1175/1520-0493(1994)122%3c2573:AGMFTA%3e2.0.CO;2

Hodges KI (1995) Feature tracking on the unit sphere. Mon Weather Rev 123(12):3458–3465. https://doi.org/10.1175/1520-0493(1995)123%3c3458:FTOTUS%3e2.0.CO;2

Hodges KI (1999) Adaptive constraints for feature tracking. Mon Weather Rev 127:1362–1373. https://doi.org/10.1175/1520-0493(1999)127%3c1362:ACFFT%3e2.0.CO;2

Hoffmann P, Reinhart V, Rechid D, de Noblet-Ducoudré N, Davin EL, Asmus C, Bechtel B, Böhner J, Katragkou E, Luyssaert S (2022) High-resolution land use and land cover dataset for regional climate modelling: historical and future changes in Europe. Earth Syst Sci Data Discuss 15:3819–3852. https://doi.org/10.5194/essd-15-3819-2023

Holtslag A, de Bruijn E, Pan HL (1990) A high resolution air mass transformation model for short-range weather forecasting. Mon Weather Rev 118:1561–1575

Hong S-Y, Dudhia J, Chen S-H (2004) A revised approach to ice microphysical processes for the bulk parameterization of clouds and precipitation. Mon Weather Rev 132:103–120

Hostetler SW, Bates GT, Giorgi F (1993) Interactive nesting of a lake thermal model within a regional climate model for climate change studies. J Geophys Res 98:5045–5057

Isotta F, Frei C, Weilguni V, Perčec Tadić M, Lassegues P, Rudolf B, Pavan V, Cacciamani C, Antolini G, Ratto S, Munari M, Micheletti S, Bonati V, Lussan C, Ronchi C, Panettieri E, Marigo G, Vertačnik G (2014a) The climate of daily precipitation in the Alps: development and analysis of a high-resolution grid dataset from pan-Alpine rain-gauge data. Int J Climatol 34(5):1657–1675. https://doi.org/10.1002/joc.3794

Isotta F, Frei C, Weilguni V, Perčec Tadić M, Lassegues P, Rudolf B, Pavan V, Cacciamani C, Antolini G, Ratto S, Munari M, Micheletti S, Bonati V, Lussan C, Ronchi C, Panettieri E, Marigo G, Vertačnik G (2014b) EURO4M-APGD (Version 2.0). https://doi.org/10.18751/Climate/Griddata/APGD/1.0

Iturbide M, Gutiérrez JM, Alves L, Bedia J, Cerezo-Mota R, Di Luca A, Faria SH, Gorodetskaya I, Hauser M, Herrera S, Hennessy KJ, Jones R, Krakovska S, Manzanas R, Martínez-Castro D, Narisma GT, Pinto I, Seneviratne SI, van den Hurk B, Vera CS (2020) An update of IPCC physical climate reference regions for subcontinental analysis of climate model data: definition and aggregated datasets. Earth Syst Sci Data 12(4):2959–2970. https://doi.org/10.5194/essd-12-2959-2020

Johansson B (2000) Areal precipitation and temperature in the Swedish Mountains. An evaluation from a hydrological perspective. Nord Hydrol 31:207–228

Kain JS (2004) The kain-fritsch convective parameterization: an update. J Appl Meteorol 43(1):170–181

Kiehl J, Hack J, Bonan G, Boville B, Breigleb B, Williamson D, Rasch P (1996) Description of the NCAR community climate model (CCM3). National center for atmospheric research tech note NCAR/TN-420+STR. NCAR, Boulder CO

Knapp KR, Kruk MC, Levinson DH, Diamond HJ, Neumann CJ (2010) The international best track archive for climate stewardship (IBTrACS): unifying tropical cyclone best track data. Bull Am Meteor Soc 91:363–376. https://doi.org/10.1175/2009BAMS2755.1

Knapp KR, Diamond HJ, Kossin JP, Kruk MC, Schreck CJ (2018) International best track archive for climate stewardship (IBTrACS) project, version 4. NOAA National Centers for Environmental Information. https://doi.org/10.25921/82ty-9e16. Accessed 10 Sept 09 2019

Kreklow J, Tetzlaff B, Burkhard B, Kuhnt G (2020) Radar-based precipitation climatology in Germany-developments, uncertainties and potentials. Atmosphere 11:217. https://doi.org/10.3390/atmos11020217

Kummerow C, Simpson J, ThielE O, BARNES W, CHANG ATC, STOCKER E, NAKAMURA K (2000) The status rainfall measuring mission (TRMM of the tropical) after two years in orbit. J Appl Meteorol Climatol 39(12):1965–1982. https://doi.org/10.1175/1520-0450(2001)040%3c1965:TSOTTR%3e2.0.CO;2.

Lewis E, Quinn N, Blenkinsop S, Fowler HJ, Freer J, Tanguy M, Woods R (2018) A rule based quality control method for hourly rainfall data and a 1 km resolution gridded hourly rainfall dataset for Great Britain: CEH-GEAR1hr. J Hydrol 564:930–943

Lewis E, Quinn N, Blenkinsop S, Fowler HJ, Freer J, Tanguy M, Hitt O, Coxon G, Bates P, Woods R, Fry M, Chevuturi A, Swain O, White SM (2022) Gridded estimates of hourly areal rainfall for great britain 1990–2016 [CEH-GEAR1hr] v2. NERC EDS Environ Inf Data Centre. https://doi.org/10.5285/fc9423d6-3d54-467f-bb2b-fc7357a3941f

Liang X-Z, Wu X (2005) Evaluation of a GCM subgrid cloud-radiation interaction parameterization using cloud-resolving model simulations. Geophys Res Lett 32:6801. https://doi.org/10.1029/2004GL022301

Lipzig NPV, Walle JVD, Belušić D, Berthou S, Coppola E, Demuzere M, Thiery W (2023) Representation of precipitation and top-of-atmosphere radiation in a multi-model convection-permitting ensemble for the Lake Victoria Basin (East-Africa). Climate Dyn 60(11):4033–4054. https://doi.org/10.1007/s00382-022-06541-5

Liu L, Solmon F, Vautard R, Hamaoui-Laguel L, Torma CZ, Giorgi F (2016) Ragweed pollen production and dispersion modelling within a regional climate system, calibration and application over Europe. Biogeosciences 13:2769–2786

Malguzzi P, Grossi G, Buzzi A, Ranzi R, Buizza R (2006) The 1966 "century" flood in Italy: a meteorological and hydrological revisitation. J Geophys Res 101(D24):D24106. https://doi.org/10.1029/2006jd007111

Mlawer EJ, Taubman SJ, Brown PD, Iacono MJ, Clough SA (1997) RRTM, a validated correlated-k model for the longwave. J Geophys Res Atmos 102(D14):16663–16682

Mlawer EJ, Clough SA (1997b) On the extension of rapid radiative transfer model to the shortwave region. In: Proceedings of the 6th atmospheric radiation measurement (ARM) science team meeting, U.S. Department of Energy, CONF-9603149

Mohr M (2009) Comparison of versions 11 and 10 of gridded temperature and precipitation data for Norway. Nor Meteorol Inst 19:475

Nogherotto R, Tompkins AM, Giuliani G, Coppola E, Giorgi F (2016) Numerical framework and performance of the new multiple-phase cloud microphysics scheme in RegCM4.5: precipitation, cloud microphysics, and cloud radiative effects. Geosci Model Dev 9:2533–2547

Oleson KW, Lawrence DM, Bonan GB, Drewniak B, Huang M, Koven CD, Yang ZL (2013) Technical description of version 45 of the community land model (CLM). Ncar technical note NCAR/TN-503+STR. National Center for Atmospheric Research, Boulder, CO, p 422

Pal JS, Small EE, Eltahir EAB (2000) Simulation of regional-scale water and energy budgets: representation of subgrid cloud and precipitation processes within RegCM. J Geophys Res 105:29579–29594

Pal JS, Giorgi F, Bi X, Elguindi N, Solmon F, Gao X, Zakey A (2007) The ICTP RegCM3 and RegCNET: regional climate modeling for the developing world. Bull Am Meteorol Soc 88:1395–1409

Pichelli E, Coppola E, Sobolowski S, Ban N, Giorgi F, Stocchi P et al (2021) The first multi-model ensemble of regional climate simulations at kilometer-scale resolution part 2: historical and future simulations of precipitation. Climate Dyn 56(11–12):3581–3602. https://doi.org/10.1007/s00382-021-05657-4

Ratnam JV, Giorgi F, Kaginalkar A et al (2009) Simulation of the Indian monsoon using the RegCM3–ROMS regional coupled model. Clim Dyn 33:119–139

Rauthe M, Steiner H, Riediger U, Mazurkiewicz A, Gratzki A (2013) A central European precipitation climatology–part I: generation and validation of a high-resolution gridded daily data set (HYRAS). Meteorol Z 22(3):235–256

Reale M, Giorgi F, Solidoro C, Di Biagio V, Di Sante F, Mariotti L et al (2020) The regional earth system model RegCM-ES: evaluation of the Mediterranean climate and marine biogeochemistry. J Adv Model Earth Syst 12:e2019MS001812

Reboita MS, da Rocha RP, Ambrizzi T, Sugahara S (2010) South Atlantic Ocean cyclogenesis climatology simulated by regional climate model (RegCM3). Clim Dyn 35(7–8):1331–1347. https://doi.org/10.1007/s00382-009-0668-7

Shalaby A, Zakey AS, Tawfik AB, Solmon F, Giorgi F, Stordal F, Sillman S, Zaveri RA, Steiner AL (2012) Implementation and evaluation of online gas-phase chemistry within a regional climate model (RegCM-CHEM4). Geosci Model Dev 5:741–760

Shi Y, Yu M, Erfanian A, Wang G (2018) Modeling the dynamic vegetation-climate system over China using a coupled regional model. J Climate 31(15):6027–6049

Sitz LE, di Sante F, Fantini R, Fuentes-Franco R, Coppola E, Mariotti L et al (2017) Description and evaluation of the earth system regional climate model (RegCM-ES). J Adv Model Earth Syst 9(4):1863–1886. https://doi.org/10.1002/2017ms000933

Schamm K, Ziese M, Becker A, Finger P, Meyer-Christoffer A, Schneider U, Schröder M, Stender P (2014) Global gridded precipitation over land: a description of the new GPCC first guess daily product. Earth Syst Sci Data 6:49–60. https://doi.org/10.5194/essd-6-49-2014

Schneider U, Hänsel S, Finger P, Rustemeier E, Ziese M (2022) GPCC full data monthly product version 2022 at 0.25: monthly land-surface precipitation from rain-gauges built on GTS-based and historical data. https://doi.org/10.5676/DWD_GPCC/FD_M_V2022_025

Solmon F, Giorgi F, Liousse C (2006) Aerosol modeling for regional climate studies: application to anthropogenic particles and evaluation over a European/African domain. Tellus B Chem Phys Meteorol 58(1):51–72

Solmon F, Mallet M, Elguindi N, Giorgi F, Zakey A, Konaré A (2008) Dust aerosol impact on regional precipitation over western Africa, mechanisms and sensitivity to absorption properties. Geophys Res Lett 35:L24705. https://doi.org/10.1029/2008GL035900

Steiner AL, Pal JS, Rauscher SA, Bell JL, Diffenbaugh NS, Boone A, Giorgi F (2009) Land surface coupling in regional climate simulations of the West Africa monsoon. Climate Dyn 33:869–892

Sundqvist H (1988) Parametrization of condensation and associated clouds in models for weather prediction and general circulation simulation. In: Schlesinger ME (ed) Physically-based modelling and simulation of climate and climate change. Kluwer, Alphen aan den Rijn, pp 433–461

Szalai S, Auer I, Hiebl J, Milkovich J, Radim T, Stepanek P, Zahradnicek P, Bihari Z, Lakatos M, Szentimrey T, Limanowka D, Kilar P, Cheval S, Deak GY, Mihic D, Antolovic I, Mihajlovic V, Nejedlik P, Stastny P, Mikulova K, Nabyvanets I, Skyryk O, Krakovskaya S, Vogt J, Antofie T, Spinoni J (2013) Climate of the greater carpathian region. Final technical report. Available at www.carpatclim-eu.org/pages/download/

Tabary P, Dupuy P, L'henaff G, Gueguen C, Moulin L, Laurantin O, Merlier C, Soubeyroux JM (2012) A 10-year (1997–2006) reanalysis of quantitative precipitation estimation over France: methodology and first results. Weather Radar Hydrol 351:255–260

Teichmann C, Jacob D, Remedio AR, Remke T, Buntemeyer L, Hoffmann P, Im ES (2021) Assessing mean climate change signals in the global CORDEX-CORE ensemble. Clim Dyn 57:1269–1292. https://doi.org/10.1007/s00382-020-05494-x

Tiedtke M (1989) A comprehensive mass-flux scheme for cumulus parameterization in large-scale models. Mon Weather Rev 117:1779–1800

Trini Castelli S, Bisignano A, Donateo A, Landi TC, Martano P, Malguzzi P (2020) Evaluation of the turbulence parameterization in the MOLOCH meteorological model. Q J R Meteorol Soc 146:124–141

Wu J, Gao XJ (2013) A gridded daily observation dataset over China region and comparison with the other datasets. Chin J Geophys 56(4):1102–1111

Wüest M, Frei C, Altenhoff A, Hagen M, Litschi M, Schär C (2010) A gridded hourly precipitation dataset for Switzerland using rain-gauge analysis and radar-based disaggregation. Int J Climatol 30(12):1764–1775

Xu K-M, Randall DA (1996) A semiempirical cloudiness parameterization for use in climate models. J Atmos Sci 53:3084–3102

Xu Y, Gao X, Shen Y, Xu C, Shi Y, Giorgi A (2009) A daily temperature dataset over China and its application in validating a RCM simulation. Adv Atmos Sci 26:763–772

Yatagai A, Arakawa O, Kamiguchi K, Kawamoto H, Nodzu MI, Hamada A (2009) A 44-year daily gridded precipitation dataset for Asia based on a dense network of rain gauges. Sola 5:137–140. https://doi.org/10.2151/sola.2009-035

Zakey AS, Solmon F, Giorgi F (2006) Implementation and testing of a desert dust module in a regional climate model. Atmos Chem Phys 6:4687–4704

Zakey AS, Giorgi F, Bi X (2008) Modeling of sea salt in a regional climate model: fluxes and radiative forcing. J Geophys Res 113:D14221. https://doi.org/10.1029/2007JD009209

Zeng X, Zhao M, Dickinson RE (1998) Intercomparison of bulk aerodynamic algorithms for the computation of sea surface fluxes using TOGA COARE and TAO data. J Climate 11:2628–2644

Zeng X, Beljaars A (2005) A prognostic scheme of sea surface skin temperature for modeling and data assimilation. Geophys Res Lett 32:L14605. https://doi.org/10.1029/2005GL023030